



1 **Seasonal variation of atmospheric particle number**
2 **concentrations, new particle formation and atmospheric**
3 **oxidation capacity at the high Arctic site Villum Research**
4 **Station, Station Nord**

5

6 Q.T. Nguyen^{1,2,3}, M. Glasius^{2,4}, L.L. Sørensen^{1,6}, B. Jensen¹, H. Skov^{1,5,6}, W. Birmili⁷, A.
7 Wiedensohler⁷, A. Kristensson⁸, J.K. Nøjgaard¹ and A. Massling^{1,6}

8 ¹Department of Environmental Science, Aarhus University, 4000 Roskilde, Denmark

9 ²Department of Chemistry, Aarhus University, 8000 Aarhus, Denmark

10 ³Department of Engineering, Aarhus University, 8200 Aarhus, Denmark

11 ⁴Interdisciplinary Nanoscience Center (iNANO), Aarhus University, 8000 Aarhus, Denmark

12 ⁵Institute of Chemical Engineering and Biotechnology and Environmental Technology, University
13 of Southern Denmark, 5230 Odense, Denmark

14 ⁶Arctic Research Centre, Aarhus University, 8000 Aarhus, Denmark

15 ⁷Leibniz Institute for Tropospheric Research, 04318 Leipzig, Germany

16 ⁸Department of Physics, Lund University, Sweden

17

18 Correspondence to: Q.T. Nguyen (quynh@eng.au.dk)

19

20 **Abstract**

21 This work presents an analysis of the physical properties of sub-micrometer aerosol particles
22 measured at the high Arctic site Villum Research Station, Station Nord (VRS), northeast Greenland
23 between July 2010 and February 2013. The study focus on particle number concentrations, particle
24 number size distributions, the occurrence of new particle formation (NPF) events and their
25 seasonality in the high Arctic, where observations and characterization of such aerosol particle
26 properties and corresponding events are rare and understanding of related processes is lacking.



1 A clear accumulation mode was observed during the darker months from October until mid-May,
2 which became considerably more pronounced during the prominent Arctic haze months from March
3 to mid-May. In contrast, only nucleation and Aitken-mode particles were observed during the
4 summer months. Analysis of wind direction and wind speed indicated possible contributions of
5 marine sources from the easterly side of the station to the observed summertime particle number
6 concentrations, while southwesterly to westerly winds dominated during the darker months. NPF
7 events lasting from hours to days were mostly observed from June until August, with fewer events
8 observed during the months with less sunlight March, April, September, and October. It was
9 observed that ozone (O_3) is likely to play an important role in the formation and growth of new
10 particles at the site during summertime. Calculations of air-mass back trajectories using the Hybrid
11 Single Particle Lagrangian Integrated Trajectory (HYSPPLIT) model for the NPF event days
12 suggested that the events possibly originated from other places and transported together with O_3 in
13 air parcels from different heights of the boundary layer down to the station at ground level. A map
14 of event occurrence probability was computed, indicating that southerly air masses from over the
15 Greenland Sea were more likely linked to those events.

16 1. Introduction

17 Climate change driven by anthropogenic greenhouse gas emissions is a global challenge. In the
18 Arctic, the warming climate has already led to an earlier onset of spring-ice melt, later freeze-up
19 and decreasing sea-ice extent (Zwally et al., 2002; Markus et al., 2009; Stroeve et al., 2012). The
20 reduction of the Earth's albedo due to ice loss subsequently impacts the radiative balance of the
21 Earth through a positive feedback, leading to further warming. As a result, the Arctic has been
22 considered a manifestation of global warming with the rate of temperature increase in the region
23 being twice as high as the rest of the world (IPCC, 2013; ACIA, 2005), up to 8 - 9 °C along the east
24 coast of Greenland (Stendel et al., 2008). In addition to long-lived greenhouse gases, short-lived
25 climate forcers including tropospheric ozone, aerosols and black carbon also play a significant role
26 affecting the radiative balance in the Arctic (Quinn et al., 2008; Bond et al., 2013; IPCC, 2013).

27 Aerosol particles influence the radiative balance in the Arctic in many ways, through their ability to
28 absorb and scatter incoming solar radiation or by acting as cloud condensation nuclei to form cloud
29 and fog droplets. The presence of low level liquid clouds above bright ice- and snow-covered
30 surfaces in the Arctic could lead to increasing near-surface temperature as opposed to a cooling
31 effect observed in most other global regions (Shupe and Intrieri, 2004; Bennartz et al., 2013),
32 though the effect is probably small (AMAP, 2011). At the same time, deposition of black carbon on
33 Arctic snow- and ice-covered surfaces accelerates surface heating and ice melting in early spring



1 (Hansen and Nazarenko, 2004; Flanner et al., 2007; Flanner et al., 2009). It is thus crucial to
2 investigate the dynamics of atmospheric aerosol particles observed in the Arctic (involving the
3 formation, concentration, physico-chemical properties, temporal variability and transport) to
4 understand their direct and indirect effects on the radiation budget.

5 It is well known that during each winter extending into spring, Arctic aerosol particles containing
6 mineral dust, black carbon, heavy metals, elements, sulfur and nitrogen compounds are detected in
7 elevated concentrations. This has been attributed to the annually recurring Arctic haze phenomenon,
8 which is related to distant latitude anthropogenic pollution (Li and Barrie, 1993; Quinn et al., 2002;
9 Ström et al., 2003; Heidam et al., 2004; Heidam et al., 1999; Nguyen et al., 2013). The focus was
10 thus on long-range transported aerosols, which are expected to be aged due to the long transport
11 distance from mid-latitude source regions.

12 A number of studies have reported in-situ formation of new aerosol particles in the Arctic, which
13 mostly involved new particle formation in the Arctic boundary layer. The first observations of the
14 occurrence of an ultrafine particle mode (< 20 nm) in the Arctic marine boundary layer during
15 summer and autumn were reported by Wiedensohler et al. (1996) and Covert et al. (1996).
16 Observations of small aerosol particles during the summer period have also been reported at the
17 Zeppelin mountain site, Svalbard (11.9°E, 78.9°N, 478 m a.s.l.) within the Arctic boundary layer
18 (Ström et al., 2003; Tunved et al., 2013). The current understanding on mechanisms of new particle
19 formation in the marine boundary layer over the Arctic Ocean is unclear, due to the low
20 concentration of nucleating agents such as sulfuric acid in the marine boundary layer (Pirjola et al.,
21 2000; Karl et al., 2012), in addition to the limited number of observational data. Growth of ultrafine
22 particles has been observed at Summit, Greenland (38.4°W, 72.6°N, 3200 m a.s.l.) (Ziembra et al.,
23 2010). Quinn et al. (2002) also found an increase in particle number concentrations during the
24 summer months at Barrow, Alaska (156.6°W, 71.3°N, 8 m a.s.l.), which was attributed to the
25 formation of smaller particles. A correlation between summertime particle number concentrations
26 and the biogenic production of methane sulfonate (MSA⁻) was shown, indicating that the production
27 of summertime particles may be associated with biogenic sulfur (Quinn et al., 2002). Similar
28 finding has been recently reported by Leaitch et al. (2013) based on observations from Alert,
29 Nunavut. Heintzenberg et al. (2015) observed newly formed small aerosol particles during several
30 cruises to the summer central Arctic Ocean and suggested that they could originate from around the
31 Arctic region, more specifically related to air masses passing by open waters prior to the
32 observation point.

33 Meanwhile, source regions of aerosol particles in the Arctic could be very different (Hirdman et al.,
34 2010). Barrow is mostly influenced by North America and Arctic basin with some Russian and



1 Siberian sources (Quinn et al., 2002). Summit, which is located above the planetary boundary layer,
2 receives frequent long-range transported pollution from North America and extensively from
3 Eurasia during wintertime (Kahl et al., 1997; Hirdman et al., 2010). The mountainous site Zeppelin
4 (Tunved et al., 2013) and the ground level site VRS (16°40'W, 81°36'N, 30 m a.s.l.) (Heidam et al.,
5 2004; Nguyen et al., 2013) both receive long range transported pollution predominantly from
6 Eurasia during winter and spring. Zeppelin is often located south of the Polar Front receiving
7 transport from the Atlantic Ocean during summer (Tunved et al., 2013). Svalbard is also influenced
8 by the Gulf Stream (Pnyushkov et al., 2013) and surrounded by open sea during summertime. VRS
9 is influenced by the ice stream from the Arctic Ocean along the east coast of Greenland (Stendel et
10 al., 2008; Kwok, 2009) and surrounded by multi-year sea ice, with limited first-year ice along the
11 coast. Such differences could have considerable impacts on NPF events and also aerosol particle
12 properties, which requires investigations at high spatial resolution in the Arctic.

13 VRS, Station Nord is a unique coastal station located close to sea level, representing the conditions
14 of the high Arctic throughout the year. Until date, there is only one observation and characterization
15 of NPF events at Alert, Nunavut (Leitch et al., 2013), while understanding of particle size
16 distribution, seasonality as well as related mechanisms and processes of NPF events are lacking
17 from such a high Arctic site.

18 This study aims to characterize the formation, concentration, physical properties and seasonality of
19 atmospheric aerosols based on particle number size distributions at VRS. The occurrence of NPF
20 events was investigated in details. The events were classified and analyzed together with ozone (O₃)
21 and nitrogen oxides (NO_x = NO + NO₂). Wind direction and wind speed were analyzed to
22 investigate the impacts of source regions on the observed seasonality of particle number size
23 distribution. The source regions of new particle formation were mapped based on calculations of air
24 mass back trajectories using the HYSPLIT model during event days and non-event days. A
25 probability map for NPF event occurrence was computed.

26 **2. Methods**

27 **2.1. Measurement site**

28 Aerosol particles and trace gases were measured at the measurement site “Flyger’s Hut”, VRS,
29 Station Nord in northeast Greenland (81°36'N, 16°40'W, 30 m a.s.l.). The site is located on a small
30 peninsula (Princess Ingeborgs Peninsula) at approximately 2.5 km southeast of a small Danish
31 military base housing a crew of five soldiers (**Fig. 1**). Electricity at “Flyger’s Hut” is supplied from
32 a local JET A-1 fuel generator located inside the military base. The remote location of the station
33 implies a minor, though unavoidable, contribution of local anthropogenic pollution originating from



1 the military camp. The station is surrounded by multi-year sea ice, with limited bare ground
2 occasionally and limited first-year ice along the coast of Greenland during the summer months. At
3 VRS, Station Nord, polar sunrise is observed in the end of February, while polar day prevails from
4 mid-April to the beginning of September and polar night prevails from mid-October to the end of
5 February.

6 **2.2. Instrumentation**

7 **2.2.1. Mobility Particle Size Spectrometer**

8 Measurement of particle number size distributions at Station Nord was initiated in July 2010 using a
9 TROPOS-type Mobility Particle Size Spectrometer as described in Wiedensohler et al. (2012).
10 Briefly, the instrument consists of a medium Vienna-type Differential Mobility Analyzer (DMA)
11 followed by a butanol-based Condensation Particle Counter (CPC 3772 by TSI Inc., Shoreview,
12 USA). The DMA design is described in Winklmayr et al. (1991). The system is operated at 1 l min^{-1}
13 aerosol flow rate and 5 l min^{-1} sheath air flow rate. The DMA sheath flow is circulated in closed
14 loop, facilitated by a regulated air blower. This technical setup allows measurements across a
15 particle size range from 10 to 900 nm in diameter. The time resolution of the instrument is 5 min,
16 including up-scan and down-scan.

17 The instrument was specifically designed to allow long-term operation with minimum maintenance
18 as follows. The DMA sheath air flow rate was continuously measured using a calibrated mass flow
19 sensor. The DMA aerosol flow rate was monitored by a pressure drop measurement over a
20 calibrated capillary. A computer-based control program adjusted the sheath air flow rate after each
21 measurement of the particle number size distribution. Systematic deviations in the sample flow rate,
22 which was controlled by a critical orifice in the CPC were monitored and corrected for in the
23 successive size distribution evaluation. Additionally, absolute pressure was measured at the inlet of
24 the system to detect any substantial technical problems such as clogging of the inlet. Temperature
25 and relative humidity (RH) were monitored at several positions inside the instrument. The RH
26 inside the DMA is the most critical parameter, since excessive moisture would allow particles to
27 grow much beyond their nominal dry diameter. At VRS, Station Nord, RH is usually not a critical
28 issue, as the climate is cold and arid with low humidity most of the year. The temperature in the
29 laboratory is mostly considerably higher than outdoor temperature, implying that substantial drying
30 of the aerosol is not needed most of the time during sample intake into the laboratory.

31 **2.2.2. Data processing**



1 The raw particle electrical mobility distributions collected by the mobility particle size spectrometer
2 were processed by a linear inversion algorithm presented in Pfeifer et al. (2014).

3 As a first part of quality control, any data associated with DMA excess air RH above 50 % and
4 sheath air temperature above 30 °C were excluded from further data analysis, as recommended by
5 ACTRIS and WMO-GAW ([http://www.wmo-gaw-wcc-aerosol-physics.org/recommen-](http://www.wmo-gaw-wcc-aerosol-physics.org/recommendations.html)
6 [dations.html](http://www.wmo-gaw-wcc-aerosol-physics.org/recommendations.html)). These incidents were only observed on a few days during the study period.

7 Subsequently, daily particle number size distributions were plotted to inspect any sudden increase in
8 the particle number concentration above the background. If short-lived particle number
9 concentration peaked without any detectable particle growth coincided with similar peaks of NO_x,
10 they were interpreted as local pollution events and excluded from the data set. These local pollution
11 events were observed throughout the year at the station. **Fig. 2** shows the extent of data coverage
12 over the study period. Gaps in the data set (most notably in 2011) were due to excluded data with
13 flow uncertainties. 2012 was the year with the best data coverage, with the lowest percentage of ca.
14 78 % in March while exceeding 90 % in most other months. The year 2012 was therefore chosen to
15 examine the seasonality of Arctic aerosols in details.

16 **2.2.2. Gas phase and meteorological parameters**

17 O₃ was measured using an API photometric O₃ analyzer (M400). The results were averaged to a
18 time resolution of 30 min. The detection limit was 1 ppbv with an uncertainty of 3 % and 6 % for
19 measured concentrations above and below 10 ppbv, respectively. The uncertainties were calculated
20 at 95 % confidence interval.

21 NO_x was averaged to a time resolution of 30 min (Teledyne API M200AU, San Diego, CA) with a
22 precision of 5 % and a detection limit of 150 ppt. The calibration was checked weekly using 345
23 ppb NO span gas while zero gas was added each 25 hour. NO_x was sampled at a flow rate of 1 l
24 min⁻¹. Coverage of O₃ and NO_x data in this study are indicated as the corresponding blue and red
25 line in **Fig. 2**.

26 Wind speed and wind direction data were obtained from a sonic anemometer (METEK, USA-1,
27 heated) for the period from April 2011 to April 2013. In winter periods fewer data were obtained
28 due to frost on the anemometer when temperature was below approximately -35 °C.

29 **2.3. Classification of new particle formation events**



1 NPF events were identified and classified following a scheme adapted from Dal Maso et al. (2005).
2 A brief description is given here.

3 A plot was compiled for each day with available particle number size distribution data, plotting the
4 particle diameter on the y-axis, time of the day (from midnight to midnight) on the x-axis, with the
5 particle number concentration in each size interval displayed as a contour plot. A panel of three
6 persons performed visual inspection, identification and classification of data to avoid subjective
7 bias. In order to be classified as an event day, the occurrence of a new particle mode below 20 nm
8 with concentrations substantially higher than during the previous hours must be observed. If a clear
9 diameter growth of newly formed particles could be traced for several hours, that specific day
10 would be classified as a class I event day. If the growth of newly formed particles was not
11 continuous over several hours, that specific day would be classified as a class II event day. The
12 identified NPF events at Station Nord typically lasted from hours to days. In case of a multi-day
13 event, only the first day, during which the event onset was identified, was counted as an event day.
14 The panel must agree on all classifications, otherwise the specific day would be classified as an
15 undefined event. Other options for classifications are non-event day or bad data in case of missing
16 data or observed instrumental problems.

17 **3. Results and Discussion**

18 This section presents the observed overall seasonality of particle number size distributions
19 measured at VRS, Station Nord during the time period from July 2010 to February 2013, with an
20 analysis of NPF event cases together with the atmospheric oxidation capacity at the station.
21 Analysis of local wind speed, wind direction and air mass back trajectories was used to support the
22 interpretation of the seasonality of particle number size distributions and the dynamics of NPF
23 events.

24 **3.1. Particle number size distributions and seasonality**

25 **3.1.1. Overview**

26 A clear seasonality of particle number size distributions was observed during 2012 (**Fig. 3-4**). A
27 persistent accumulation mode appeared in the end of September, which became more prominent in
28 the end of February lasting until mid-May. The Arctic summer (June - August) was coupled with a
29 higher abundance of nucleation mode and Aitken mode aerosol particles and a very low abundance
30 of accumulation mode particles (Table 1). The small particles were also observed to a lesser extent



1 in September and only during one episode in mid-October. This observation of strong seasonality
2 was supported by observations from the available scattered data in the other years 2010, 2011 and
3 2013. The elevated concentrations of accumulation mode particles observed in this study generally
4 followed the varying pattern of aged total suspended particles during the Arctic haze period
5 previously reported at VRS, Station Nord (Heidam et al., 2004; Nguyen et al., 2013) and other
6 Arctic stations (Quinn et al., 2002; Ström et al., 2003). It should also be noted that the sun rises in
7 the end of February at Station Nord, so the period thereafter is affected by photochemical processes.
8 Observations of smaller particles during this period were in accordance with previous studies in the
9 Arctic (Ström et al., 2003; Tunved et al., 2013; Wiedensohler et al., 1996; Covert et al., 1996;
10 Quinn et al., 2002; Heintzenberg et al., 2015; Leaitch et al., 2013). During this period, the Arctic is
11 considerably cleaner with respect to long-range transport of atmospheric pollutants and
12 characterized by constant daylight.

13 3.1.2. Statistics of the particle number size distribution

14 **Fig. 4** and **Table 1** describe detailed statistics of the particle number size distributions measured at
15 the site, especially regarding the prominent accumulation mode during February - May and the
16 prominent nucleation/Aitken mode during June - August. **Table 2** provides detailed median and
17 average particle number concentration (N), particle volume concentration (V) and particle mass
18 concentration (M) values calculated using the particle number size distributions at VRS, Station
19 Nord during 2012. Higher values of median or average N were observed from April to September.
20 During this period, largest discrepancies between the median and the average values were also
21 found, especially during June (Median N = 137 particles cm⁻³, Average N = 277 particles cm⁻³) and
22 August (Median N = 227 particles cm⁻³, Average N = 313 particles cm⁻³). This was attributed to the
23 occurrence of intense NPF events during these months (**Fig. 3**), skewing the average N towards
24 higher values compared to median N. June and August also showed highest average N in 2012,
25 followed by May, April and July, whereas the months with the lowest average N were October,
26 November and December. Since nucleation mode particles were almost absent in April and
27 relatively minor in May, their corresponding high median or average N values observed were
28 attributed to the elevated presence of the pronounced accumulation mode during these two months
29 (**Fig. 3**).

30 Newly formed particles are usually high in number and therewith significantly influence the total
31 number concentration N as discussed above; however they do not contribute considerably to the



1 total particle volume concentration V . As a result, June and August were among the months with
2 the lowest median or average V together with other sunlit months July and September (**Table 2**). In
3 contrast, the highest median and average V were observed during the most prominent haze months
4 March - May. Simple log-normal fitting applied to the accumulation mode observed in the monthly
5 particle number size distributions in 2012 revealed a geometrical mean diameter of approximately
6 170 nm during the winter and spring months (**Table 1**). This indicates that the particles can
7 originate from distant locations due to their longer lifetimes determined by their size (Massling et
8 al., 2015).

9 The total particle mass concentrations M were derived directly from the total particle volume
10 concentration V , assuming a density of 1.4 g cm^{-3} and particle sphericity. Average monthly
11 estimates of M ranged from $0.21 \text{ } \mu\text{g m}^{-3}$ (June) to $1.58 \text{ } \mu\text{g m}^{-3}$ (March) (**Table 2**).

12 Similar distribution of the major modes was also observed at the Zeppelin mountain site by Tunved
13 et al. (2013). However, the nucleation mode - Aitken mode observed during the summer months
14 seemed considerably more pronounced at VRS, Station Nord compared to Zeppelin. This indicates
15 higher number concentrations of smaller particles at Station Nord, which were visible until October
16 (**Fig. 3-4**). In regards of the total particle mass concentration, Tunved et al. (2013) reported summer
17 M mostly below $0.2 \text{ } \mu\text{g m}^{-3}$ and higher M below $0.8 \text{ } \mu\text{g m}^{-3}$ observed at Zeppelin during the
18 prominent haze months March - April (with an assumed lower density of 1 g cm^{-3}). Clearly, the
19 particle mass concentration at Villum Research Station, VRS, Station Nord seemed comparable
20 during summer while showing higher concentrations during the Arctic haze months compared to
21 Zeppelin with different assumed particle densities already accounted for. This difference between
22 the two sites could be partially attributed to their different locations as discussed above. In addition,
23 the study periods and lengths of the studies were also different, as the Zeppelin data was averaged
24 for March 2000 - March 2010 whereas the descriptive distribution statistics in this work was
25 derived solely from data in 2012. Nevertheless, similar observations at both stations show the
26 consistent and predictable annual behavior of the particle number size distributions in the Arctic.

27 **3.1.3. Impacts of seasonal wind pattern**

28 Analysis of wind direction and wind speed was performed to investigate the impacts of wind pattern
29 on the particle number size distributions at the station. **Fig. 5** demonstrates monthly wind roses
30 during 2012, where two distinct patterns could be identified during the darker (September - April)
31 and the summer (June - August) period. The early haze months (January and February) and the



1 prominent haze months (March and April) showed prevailing wind arriving from the southwesterly
2 to westerly direction. During May, some northerly wind was observed while the frequency of
3 southwesterly wind seemed to decrease. During the summer period (June - August), when smaller
4 and freshly formed particles were observed, easterly wind became more prominent, especially
5 during July and August. September marked a prompt change in the wind direction back to
6 southwesterly direction. The wind speed became higher during November - December, which is
7 probably due to increasing katabatic winds from the ice sheet. During the other years 2011 and
8 2013 (data not shown), considerably similar patterns were observed for the corresponding months.

9 Earlier studies on source apportionment of total suspended particles (TSP) observed during the
10 Arctic haze period at VRS mostly identified Siberian industries and long-range transport from mid-
11 latitudes as major factors (Nguyen et al., 2013; Heidam et al., 2004) . However, the wind pattern
12 shown here may indicate an immediate impact of the adjacent southwesterly to westerly regions
13 contributing to the properties of particles prior to arrival at the station.

14 Based on the summer wind pattern, the smaller particles observed during June - August were
15 probably linked to sources from the easterly side of the station, with some marine contribution.
16 During summer, the marine contribution from the easterly direction is possibly driven by the retreat
17 of sea-ice cover, which exposes areas of open waters (“open leads”) and melt water on top of sea
18 ice to wind stress, especially along the coastal line of Greenland due to the presence of first-year-ice
19 in these regions. This would result in enhanced primary emissions of sea spray particles (Korhonen
20 et al., 2008). Surface active organic species in the ocean surface layer, which are more abundant due
21 to increased biological activity during summer, could also be released into the atmosphere by
22 bubble bursting (Middlebrook et al., 1998; Tervahattu et al., 2002) and become mixed with other
23 sea spray particles. It was suggested by Sellegri et al. (2006) that this could also alter the number
24 size distributions of particles. Another study by Karl et al. (2013) proposed that new nanoparticles
25 in the high Arctic could be marine granular nanogels injected into the atmosphere from evaporating
26 cloud droplets. Recent analysis of particle number size distributions and back trajectories during
27 summer cruises in the Arctic by Heintzenberg et al. (2015) also showed a high coupling of newly
28 formed particles and the traveling of air masses over open water. At the same time, it must be noted
29 that wind measurements using the sonic anemometer were confined to local observations at ground
30 level, which according to radio sound measurements by Batchvarova et al. (2013), do not capture
31 activities such as transport of air masses at higher altitudes, or transport from a broader region. The
32 extent of wind impacts on the particle size distributions at the station is thus not well constrained.



1 Previous studies reported a dependence of particle number concentrations on wind speed in the
2 Arctic (Leck et al., 2002) and North Atlantic (Odowd and Smith, 1993). However, in this study the
3 accumulation mode particles (110 - 900 nm) only showed positive correlation with wind speed
4 during eight out of 12 months of 2012 with a moderate Pearson correlation coefficient range of 0.05
5 - 0.38. The reason could be partly attributed to the larger size ranges (500 nm up to 16 μm in
6 diameter) measured in the other studies, which are more influenced by wind speed.

7 **3.2. New particle formation events**

8 **3.2.1. Description of exemplary NPF events**

9 NPF events were observed at the station during the sunlit months, especially during the summer
10 months June – August, though events were also identified during the months with relatively low
11 sunlight March and October. The onset of NPF events was observed during various hours of the day
12 during the summer months, in combination with very small variations in solar flux during the day.
13 Examples of three events were shown in **Fig. 6**. As apparent from the figure, the events showed
14 clear but slow growth over considerably long periods up to a few days.

15 **3.2.2. The role of atmospheric oxidants**

16 **Fig. 6** also shows an overlay of O_3 , NO and NO_x on the NPF event plots to allow analysis of the
17 role of atmospheric oxidants during those events.

18 **Ozone**

19 O_3 shows a strong seasonality in the Arctic troposphere with maximum springtime concentration
20 observed in the free troposphere, which is however poorly understood (Monks, 2000; Law and
21 Stohl, 2007). It has long been indicated that tropospheric O_3 in the Arctic is enriched from intruding
22 stratospheric air masses (Gregory et al., 1992; Gruzdev and Sitnov, 1993). A recent model study has
23 also suggested that summertime photochemical production of O_3 by NO_x in the Arctic could also be
24 a dominant source (Walker et al., 2012). This was attributed to NO_x emissions from the thermal
25 decomposition of the long-lived reservoir species peroxyacetyl nitrate (PAN) during summer (Fan
26 et al., 1994). Meanwhile, transport from mid-latitude source regions could also contribute to the O_3
27 budget in the Arctic during autumn and winter (Walker et al., 2012). Sources of O_3 in the Arctic
28 could therefore be a combination of different factors, including among others stratospheric
29 influence, local production and transport from mid-latitude sources. Finally, surface O_3 is also



1 depleted every spring due to reactions with Br atoms (Barrie et al., 1988; Simpson et al., 2007;
2 Skov et al., 2004), similar to O₃ depletion in the stratosphere.

3 In this work, O₃ was used as a tracer of atmospheric chemical processes, and the concentration of
4 O₃ was found to be related to the formation and growth of new particles at Station Nord during
5 summer based on case studies of NPF events in 2012 (**Fig. 9**).

6 **Event A, Fig. 6:** Event A is in fact a “double” event, with the first event occurring over June 15 - 16
7 followed by another event starting on June 17 with traceable growth until June 20.

8 During June 15, the O₃ level (black line) increased considerably to ~45 ppbv, which was
9 significantly higher than the average summer (June - August, 2012) concentration of O₃ (~26 ppbv).
10 As the NPF event on June 15 started followed by particle growth up to ~25 nm, the O₃ level
11 dropped dramatically, then somewhat stabilized when the approximate mean particle size reaches
12 the lower Aitken mode. The next drop in O₃ concentration (from ~37 ppbv to ~27 ppbv) coincided
13 with the occurrence of the second NPF event observed around noon of June 17. As the new particles
14 grew beyond ~30 nm in diameter, the O₃ concentration seemed to stabilize again.

15 In the late hours of June 19, the O₃ concentration suddenly dropped by ~5 ppbv, coinciding with an
16 interruption of the event. By midday June 20, the O₃ concentration increased back to the pre-
17 interruption level, while that interrupted event also seemed to be brought back to the station. It was
18 unclear if this drop of O₃ concentration on June 19 was associated with any NPF, as nucleation
19 sized particles were also observed for a few hours during early hours on June 20. However, a full
20 justification of this observation was not possible due to the detection limit of the Mobility Particle
21 Size Spectrometer system (~10 nm) confining to only aged nucleation particles. Another
22 explanation could be that both O₃ and the nucleation event were transported to the station from a
23 common source, with the interruption probably indicating for instance a displacement of air mass.

24 It has been observed that O₃ depletion occurs only when filterable bromide fBr is present, which is
25 in agreement with the evidence that O₃ is removed by Br atoms (Skov et al., 2004; Goodsite et al.,
26 2004; Goodsite et al., 2013). NPF at coastal location has also been found related to iodine oxides
27 (O'Dowd et al., 2002; McFiggans et al., 2010; Mahajan et al., 2011; Saiz-Lopez and von Glasow,
28 2012). This study was however unable to investigate the possible impact of halogen chemistry, due
29 to a lack of relevant measurement data.

30 During *Event A* case study, the NO and NO_x level remained mostly below 0.1 ppbv. This was
31 approximately the background level of NO_x at Station Nord throughout the year. NO and NO_x



1 concentration did not seem to relate to O₃ concentration level, or observations of new particle
2 formation events.

3 **Event B, Fig. 6:** This *Event B* on August 2 showed that a lower level of O₃ concentration (~25
4 ppbv) could also be associated with a new particle formation event. During the event, the episode of
5 traceable particle growth lasted for approximately 12h, coinciding with a concurrent drop of the O₃
6 concentration. This event was also considerably less intensive in regards of particle number
7 concentrations compared to *Event A*. Until the end of the event, particles were mostly below 30 nm
8 in size.

9 **Event C, Fig. 6:** During this event on August 9 - 10, new particle formation was also observed
10 together with lower O₃ concentrations (~25 ppbv), which was similar to *Event B*. The anti-
11 correlation between growth of newly formed particles and O₃ concentration was also observed
12 during this event. However, such anti-correlation was visible until particles almost reached 40-50
13 nm in diameter, which was higher than that observed during *Event A* and *Event B*. The growth
14 seemed to be interrupted in the morning of August 10, allowing the concentration of the O₃ oxidant
15 to recover during that exact period back to values above 25 ppbv.

16 As demonstrated with the three events, the concentration level of O₃ seemed to display an anti-
17 correlation with early particle growth up to about 30 nm during *Event A* and *Event B* or about 40-50
18 nm in case of *Event C*. It is generally agreed that particle nucleation involves sulfuric acid (H₂SO₄)
19 via the oxidation of SO₂ by the hydroxyl (OH) radical (Kulmala et al., 2001), while particle growth
20 depends considerably on vapor uptake and condensation of low-volatile organic vapor products
21 produced by photo-oxidation of volatile organic compounds (VOCs) (Donahue et al., 2011;
22 Riipinen et al., 2011; Riipinen et al., 2012). Naturally, O₃ is a major atmospheric oxidant, which
23 also undergoes photolysis to form the OH radical oxidant. These oxidants oxidize VOCs to form a
24 variety of low-volatile products. A reduction of O₃ could thus be an indirect indicator of increased
25 availability and thus uptake of low-volatile compounds, contributing to particle growth. Meanwhile,
26 it should also be noted that the role of halogen chemistry contributing to new particle formation is
27 unknown, due to a lack of relevant data as discussed above.

28 The source of VOCs at VRS, Station Nord is unclear. There might be some biogenic emissions of
29 VOCs at the station during summer, expected due to retreated snow and ice cover, exposed bare
30 ground and thus possibly increased biogenic activity. However, since this area is arid, this is
31 expected to be extremely limited. Meanwhile, the presence of VOC oxidation products such as



1 organic acids and organosulfates at the station has been reported by Hansen et al. (2014), though at
2 very low concentrations. The low mass loading of organic materials (Nguyen et al., 2014) and total
3 suspended particles (Nguyen et al., 2013) observed at the station during summer would inhibit
4 removal of small particles by coagulation, thus allowing particle growth and prolonged NPF events.

5 As O₃ only seemed to inversely correlate with particle growth up to aged nucleation or lower-
6 Aitken size, poor correlations were obtained between O₃ concentration and particle number
7 concentrations. Although the summer months in 2012 were event-active, the Pearson correlation
8 coefficients between O₃ concentrations and particle number concentrations during June, July and
9 August were 0.37, 0.26 and -0.16, respectively. Meanwhile, it was found that O₃ correlated
10 positively with the observed particle volume concentrations during June (0.80), July (0.57), August
11 (0.38) and September (0.50), which probably indicated that oxidation by O₃ was no longer
12 important as particles reached larger size. At the same time, the possibility of the O₃ oxidant and/or
13 the new particle formation events being transported to the site in the same or different air masses
14 cannot be eliminated and will be examined further using HYSPLIT analysis.

15 NO_x

16 As mentioned above, sparks of particle formation, which did not grow further, were considered as
17 local pollution events, which related to NO_x emitted by the car engine during service of the station.
18 There was probably some additional contribution from emissions from the military base, which is
19 located at a distance of about 2.5 km from the measurement site. An example of such interference is
20 illustrated during the early hours of August 2 (*Event B*, **Fig. 6**), during which a higher NO_x
21 concentration of ~0.15 ppbv was detected together with a short episode of new particle formation
22 without further growth. Such interference could also be observed around midday of the same event
23 day (*Event B*, **Fig. 6**). In contrast, it must be noted that NO_x concentrations in the range ~0.1-0.2
24 ppbv were mostly not associated with any noticeable observations of new particle formation.

25 During the late winter - spring months (March - May), episodes of depletion or complete removal of
26 the surface layer O₃ and mercury in the Arctic occur due to reaction with atmospheric bromine
27 released from sea-ice and surface snow (Barrie et al., 1988; Bottenheim et al., 1990; Pratt et al.,
28 2013; Abbatt, 2013; Abbatt et al., 2012; Skov et al., 2004). The concentration of O₃ then is so low
29 that it can no longer oxidize NO and NO₂. Local NO_x emissions thus seemed to relate to the intense
30 burst of small particles which lasted for hours. Removal of these episodes resulted in several
31 noticeable gaps in the data set, especially in March and May 2012 (**Fig. 3**).



1 The summer period June - August was associated with a lower level of background NO_x ($\text{NO}_x \sim 0.1$
2 ppbv) compared to the rest of the year ($\text{NO}_x \sim 0.2$ ppbv). NO_x emissions into the Arctic atmosphere
3 other than the direct local anthropogenic emissions could originate from the thermal decomposition
4 of PAN, which is the major atmospheric NO_x reservoir species (Singh et al., 1995). This process is
5 nevertheless limited by low temperature during winter and spring and low PAN levels during
6 summer (Beine and Krognnes, 2000). NO_x also contributes via photochemistry to the local formation
7 of tropospheric O_3 and thus enhances O_3 levels during summer (Walker et al., 2012; Beine and
8 Krognnes, 2000) at the expense of NO_x concentrations. However, a direct relation between O_3 and
9 NO_x during summertime was not observed (**Fig. 6**).

10 **3.2.3 Analysis of air mass back trajectories**

11 As mentioned above, the Mobility Particle Size Spectrometer system employed at VRS, Station
12 Nord is limited to particles larger than 10 nm in size, capturing only aged nucleation particles. It is
13 thus uncertain whether the formation of the freshly nucleated particles actually occurred at the site,
14 or if they were transported from elsewhere or produced aloft.

15 Air mass back trajectories were analyzed in order to investigate possible source regions for the
16 observed events. The trajectories were calculated using HYSPLIT (Draxier and Hess, 1998). The
17 model runs were based on meteorological data obtained from the Global Data Assimilation System
18 (GDAS), which is maintained by the US National Centers for Environmental Prediction (NCEP).

19 Air mass back-trajectories were calculated 24h to 48h backwards for air masses arriving at the
20 station at 50 m and 500 m above sea level on the event days, which were discussed earlier in **Fig. 6**.
21 The trajectories were presented in **Fig. 7**, with the names of the events kept consistent with those in
22 **Fig. 6**. Only the first two days (June 15 - 16) and the last two days (June 19 - 20) of *Event A* was
23 shown in **Fig. 7**. Calculations of air mass back trajectories were performed for these two day
24 periods, in order to minimize the uncertainties associated with calculating trajectories many days
25 backwards.

26 Descending of air parcels from above the boundary layer was commonly observed on many event
27 days, such as during *Event A* (June 15 - 16, 2012) and *Event C* (August 2, 2012) (**Fig. 7**). Strong
28 vertical mixing could relate to an interruption of an event. For example, an episode of vertical
29 mixing between the lower (red) and upper air parcels (blue) occurred around mid-day of June 19,
30 2012 and lasted until the early morning hours of the following day (~15 hours in total) (**Fig. 7**). This
31 could probably relate to the interrupted phase of particle growth and O_3 concentration earlier



1 observed (~18 hours in total) (*Event A*, **Fig. 6**). The event interruption was also observed a few
2 hours later, which was probably due to the travelled distance of the air mass between the vertical
3 displacing point above the boundary layer and that reaching the station at the ground level.
4 Nevertheless, as *Event A* resumed after the interruption on June 20, 2012, the observed lower
5 Aitken mode band seemed to continue the growth before the interruption (**Fig. 6**). Such observation
6 probably indicated that the air parcels providing the source to the new particle formation events
7 (and possibility also O₃) could be displaced from and then brought back to the station.
8 Subsequently, this could indicate that the entire event was “transported” from aloft down to the
9 ground level. Similarly, during *Event B* (August 2, 2012), vertical mixing between the upper air
10 parcels (blue) and lower air parcels (red) occurred around noon time and lasted for ~12 hours (**Fig.**
11 **7**). This seemed to relate to the NPF event occurring around the same time with roughly the same
12 length (~12 hours) (*Event B*, **Fig. 6**).

13 In fact, it was previously indicated that new particles could be formed aloft and subsequently
14 transported to the ground level due to vertical mixing, leading to new particle formation events
15 observed around noon time (Mäkelä et al., 2000; Crippa et al., 2012; Pryor et al., 2010). In another
16 study by Wiedensohler et al. (1996), it was also suggested that the observed occurrence of particles
17 smaller than 20 nm in diameter in the marine boundary layer over the Arctic pack ice could
18 originate from higher altitudes. Assuming that the new particle formation events were transferred
19 from aloft, it is possible that the vertical mixing with the upper air parcels could either interrupt an
20 event or lead to observation of a new event at the site. This would depend on whether the displaced
21 air parcels or the displacing air parcels are event-active, or having the favorable conditions for the
22 formation and growth of new particles, such as the presence of precursor gases. In contrast, an
23 observed interruption during a new particle formation event such as during the early hours of
24 August 10, 2012 (*Event C*, **Fig. 6**) was not always related to displacing air parcels. The interruption
25 could instead relate to a change in the horizontal direction of the air parcels arriving at the station
26 occurring around midnight of August 9, 2012 (**Fig. 7**).

27 Air mass back trajectories were also calculated three-days backwards, at one hour after the starting
28 time of each identified event using HYSPLIT, whereas for the other days, trajectories arriving at
29 12:00 p.m. local time were used. The region around Station Nord was split into one degree
30 latitudinal and six degree longitudinal grid boxes. Every time a trajectory passed one grid box, a
31 count was registered for that grid box. The probability of registering an event, when the air mass
32 originated from a specific grid box was obtained by dividing the total counts during event days by



1 the sum of total counts during event days, undefined and non-event days. The probability results are
2 shown in **Fig. 8**.

3 As apparent from the figure, the probability of observing an event at the station is low when the air
4 masses arrive from the southwesterly direction over Greenland. Other directions of air mass origin
5 however showed relatively similar probability of registering an event. A slightly higher probability
6 range was observed for southeasterly air masses that passed over region, where open waters and
7 melting ponds on ice are more likely to occur. As particles typically grow very slowly at Villum
8 Research Station, the time gap from particle nucleation occurring around 1.5 nm in diameter until
9 the point when they are observed at the site (~10 nm in diameter) could range from hours to days.
10 The corresponding probability for observing nucleation mode particles (~10 nm in diameter) at the
11 site should therefore serve as an indication of probable air mass origin of the grown nucleation
12 mode instead of freshly nucleated particles.

13 **3.2.4. Analysis of wind pattern during NPF events**

14 The wind pattern was also investigated on specific event days in 2011 and 2012 (figure not shown).
15 However, they were found very similar to the general wind patterns of the corresponding month or
16 period. Therefore, it is unlikely that any change in local wind direction during the specific event
17 days could have an impact on the occurrence of new particle formation events observed at the site.
18 This indicates the possibility of other factors, which may have changed during the event days
19 affecting new particle formation such as precursors. In fact, Quinn et al. (2002) indicated that the
20 abundant dimethyl sulfide (DMS) could affect particle production during summer, as evidenced by
21 a strong correlation between particle number concentrations and methanesulfonate (MSA)
22 concentrations (resulting from the oxidation of DMS). Similar observations were reported by
23 Leaitch et al. (2013). Other examples of factors influencing NPF are atmospheric oxidation capacity
24 and transport of air masses.

25 **3.2.5. Event statistics**

26 In general, the event days accounted for 15 - 38 % of the classified days during June - September,
27 with the highest percentages of event days observed in August (38 %) and July (33 %) (**Table 3**).
28 The period from June to early September was also the period during which longer events up to
29 several days were observed and most class I events were identified (**Table 3**).

30 The observed frequencies of event days during these months at VRS, Station Nord were relatively
31 higher compared to reported values from sub-Arctic stations during the same months, such as



1 Värriö (20 - 25%) (Kyro et al., 2014), Pallas (10 - 20 %) (Asmi et al., 2011) or Abisko (< 20 %)
2 (Vaananen et al., 2013). In fact, the observed new particle formation events at these stations and
3 other Nordic stations seemed to show a spring maximum of event occurrence (Vehkamaki et al.,
4 2004; Dal Maso et al., 2007; Kristensson et al., 2008), as opposed to the summer maximum of
5 events observed at VRS, Station Nord. At the same time, NPF events were still observed at the sub-
6 Arctic stations Värriö, Pallas and Abisko during the darker months (November - February), though
7 the fraction of event occurrence was typically much lower compared to other seasons (Kyro et al.,
8 2014; Asmi et al., 2011; Vaananen et al., 2013). Notably, not a single event was observed at VRS,
9 Station Nord during the Arctic night in the absence of sunlight.

10 **4. Conclusion**

11 In this work, the seasonality of particle number size distributions, total particle number, volume and
12 mass concentrations was examined. A strong seasonal pattern was found, showing the abundance of
13 smaller particles during the sunlit period of the year, especially during summer and a persistent
14 accumulation mode during the darker months caused by long-range transport of particles to the
15 Arctic. Analysis of wind data showed a dominance of easterly winds during the summer months and
16 southwesterly winds during the darker months of the year.

17 NPF events were investigated based on case studies, showing clear events lasting from hours to
18 days. O₃ was found closely related to the NPF events observed at the station, especially in regards
19 of particle growth. Calculations of air mass back trajectories on the days with new particle
20 formation events using HYSPLIT indicated an aloft origin of air parcels arriving at the station on
21 many event days. The overlaps between the occurrence of vertical displacing air masses and
22 interruption of events observed at the measurement site further suggested that the event could be
23 transported to or displaced from the site together with the air masses. Air masses arriving from the
24 southwesterly direction over Greenland were least linked to NPF event, whereas air masses arriving
25 from southeasterly direction over Greenland sea was associated with slightly higher probabilities.
26 Meanwhile, the local wind direction did not seem to relate to NPF events observed at the station

27 **Acknowledgements**

28 This work was financially supported by the Danish Environmental Protection Agency with means
29 from the MIKA/DANCEA funds for Environmental Support to the Arctic Region, which is part of
30 the Danish contribution to “Arctic Monitoring and Assessment Program” (AMAP) and to the
31 Danish research project “Short lived Climate Forcers” (SLCF). The findings and conclusions



1 presented here do not necessarily reflect the views of the Agency. This work was also supported by
2 the Nordic Centre of Excellence Cryosphere-Atmosphere Interactions in a Changing Arctic Climate
3 (CRAICC). The Villum Foundation is acknowledged for funding the construction of Villum
4 Research Station, Station Nord. The authors are also grateful to the staff at Station Nord for their
5 excellent support.

16

17



1 **References**

- 2 National Snow and Ice Data Center: <http://nsidc.org/>, access: 19 February 2016.
- 3 Abbatt, J.: Arctic snowpack bromine release, *Nat Geosci*, 6, 331-332, 2013.
- 4 Abbatt, J. P. D., Thomas, J. L., Abrahamsson, K., Boxe, C., Granfors, A., Jones, A. E., King, M. D.,
5 Saiz-Lopez, A., Shepson, P. B., Sodeau, J., Toohey, D. W., Toubin, C., von Glasow, R., Wren, S.
6 N., and Yang, X.: Halogen activation via interactions with environmental ice and snow in the polar
7 lower troposphere and other regions, *Atmos Chem Phys*, 12, 6237-6271, DOI 10.5194/acp-12-
8 6237-2012, 2012.
- 9 ACIA: (Arctic Climate Impact Assessment) Overview Report, Cambridge University Press,
10 Cambridge, 1042 p., 2005.
- 11 AMAP: Arctic Monitoring and Assessment Programme (AMAP), The Impact of Black Carbon on
12 Arctic Climate Oslo, 72, 2011.
- 13 Asmi, E., Kivekas, N., Kerminen, V. M., Komppula, M., Hyvarinen, A. P., Hatakka, J., Viisanen,
14 Y., and Lihavainen, H.: Secondary new particle formation in Northern Finland Pallas site between
15 the years 2000 and 2010, *Atmos Chem Phys*, 11, 12959-12972, DOI 10.5194/acp-11-12959-2011,
16 2011.
- 17 Barrie, L. A., Bottenheim, J. W., Schnell, R. C., Crutzen, P. J., and Rasmussen, R. A.: Ozone
18 Destruction and Photochemical-Reactions at Polar Sunrise in the Lower Arctic Atmosphere, *Nature*,
19 334, 138-141, Doi 10.1038/334138a0, 1988.
- 20 Batchvarova, E. A., Gryning, S. E., Skov, H., Sørensen, L. L., Kirova, H., and Muenkel, C.:
21 Boundary-layer and air quality study at “Station Nord” in Greenland, 33rd International Technical
22 meeting on air pollution Modelling and its applications, August 26 – 30, Miami, Florida, USA,
23 2013,
- 24 Beine, H. J., and Krognes, T.: The seasonal cycle of peroxyacetyl nitrate (PAN) in the European
25 Arctic, *Atmos Environ*, 34, 933-940, Doi 10.1016/S1352-2310(99)00288-5, 2000.
- 26 Bennartz, R., Shupe, M. D., Turner, D. D., Walden, V. P., Steffen, K., Cox, C. J., Kulie, M. S.,
27 Miller, N. B., and Pettersen, C.: July 2012 Greenland melt extent enhanced by low-level liquid
28 clouds, *Nature*, 496, 83-86, 2013.
- 29 Bond, T. C., Doherty, S. J., Fahey, D. W., Forster, P. M., Berntsen, T., DeAngelo, B. J., Flanner, M.
30 G., Ghan, S., Kärcher, B., Koch, D., Kinne, S., Kondo, Y., Quinn, P. K., Sarofim, M. C., Schultz,
31 M. G., Schulz, M., Venkataraman, C., Zhang, H., Zhang, S., Bellouin, N., Guttikunda, S. K.,
32 Hopke, P. K., Jacobson, M. Z., Kaiser, J. W., Klimont, Z., Lohmann, U., Schwarz, J. P., Shindell,
33 D., Storelvmo, T., Warren, S. G., and Zender, C. S.: Bounding the role of black carbon in the
34 climate system: A scientific assessment, *Journal of Geophysical Research: Atmospheres*, 118, 5380-
35 5552, 10.1002/jgrd.50171, 2013.
- 36 Bottenheim, J. W., Barrie, L. A., Atlas, E., Heidt, L. E., Niki, H., Rasmussen, R. A., and Shepson,
37 P. B.: Depletion of Lower Tropospheric Ozone during Arctic Spring - the Polar Sunrise Experiment
38 1988, *J Geophys Res-Atmos*, 95, 18555-18568, Doi 10.1029/Jd095id11p18555, 1990.



- 1 Covert, D. S., Wiedensohler, A., Aalto, P., Heintzenberg, J., McMurry, P. H., and Leck, C.: Aerosol
2 number size distributions from 3 to 500 nm diameter in the arctic marine boundary layer during
3 summer and autumn, *Tellus B*, 48, 197-212, 1996.
- 4 Crippa, P., Petaja, T., Korhonen, H., El Afandi, G. S., and Pryor, S. C.: Evidence of an elevated
5 source of nucleation based on model simulations and data from the NIFTy experiment, *Atmos*
6 *Chem Phys*, 12, 8021-8036, DOI 10.5194/acp-12-8021-2012, 2012.
- 7 Dal Maso, M., Kulmala, M., Riipinen, I., Wagner, R., Hussein, T., Aalto, P. P., and Lehtinen, K. E.
8 J.: Formation and growth of fresh atmospheric aerosols: eight years of aerosol size distribution data
9 from SMEAR II, Hyytiälä, Finland, *Boreal Environment Research*, 10, 323-336, 2005.
- 10 Dal Maso, M., Sogacheva, L., Aalto, P. P., Riipinen, I., Komppula, M., Tunved, P., Korhonen, L.,
11 Suur-Uski, V., Hirsikko, A., Kurten, T., Kerminen, V. M., Lihavainen, H., Viisanen, Y., Hansson,
12 H. C., and Kulmala, M.: Aerosol size distribution measurements at four Nordic field stations:
13 identification, analysis and trajectory analysis of new particle formation bursts, *Tellus B*, 59, 350-
14 361, DOI 10.1111/j.1600-0889.2007.00267.x, 2007.
- 15 Donahue, N. M., Trump, E. R., Pierce, J. R., and Riipinen, I.: Theoretical constraints on pure vapor-
16 pressure driven condensation of organics to ultrafine particles, *Geophysical Research Letters*, 38,
17 Artn L16801 Doi 10.1029/2011gl048115, 2011.
- 18 Draxier, R. R., and Hess, G. D.: An overview of the HYSPLIT_4 modelling system for trajectories,
19 dispersion and deposition, *Aust Meteorol Mag*, 47, 295-308, 1998.
- 20 Fan, S. M., Jacob, D. J., Mauzerall, D. L., Bradshaw, J. D., Sandholm, S. T., Blake, D. R., Singh, H.
21 B., Talbot, R. W., Gregory, G. L., and Sachse, G. W.: Origin of Tropospheric Nox over Sub-Arctic
22 Eastern Canada in Summer, *J Geophys Res-Atmos*, 99, 16867-16877, Doi 10.1029/94jd01122,
23 1994.
- 24 Flanner, M. G., Zender, C. S., Randerson, J. T., and Rasch, P. J.: Present-day climate forcing and
25 response from black carbon in snow, *J Geophys Res-Atmos*, 112, Artn D11202, Doi
26 10.1029/2006jd008003, 2007.
- 27 Flanner, M. G., Zender, C. S., Hess, P. G., Mahowald, N. M., Painter, T. H., Ramanathan, V., and
28 Rasch, P. J.: Springtime warming and reduced snow cover from carbonaceous particles, *Atmos*
29 *Chem Phys*, 9, 2481-2497, 2009.
- 30 Goodsite, M. E., Plane, J. M. C., and Skov, H.: A theoretical study of the oxidation of Hg-0 to
31 HgBr₂ in the troposphere, *Environ Sci Technol*, 38, 1772-1776, 10.1021/es034680s, 2004.
- 32 Goodsite, M. E., Outridge, P. M., Christensen, J. H., Dastoor, A., Muir, D., Travnikov, O., and
33 Wilson, S.: How well do environmental archives of atmospheric mercury deposition in the Arctic
34 reproduce rates and trends depicted by atmospheric models and measurements?, *Sci Total Environ*,
35 452, 196-207, 10.1016/j.scitotenv.2013.02.052, 2013.
- 36 Gregory, G. L., Anderson, B. E., Warren, L. S., Browell, E. V., Bagwell, D. R., and Hudgins, C. H.:
37 Tropospheric ozone and aerosol observations: The Alaskan Arctic, *Journal of Geophysical*
38 *Research: Atmospheres*, 97, 16451-16471, 10.1029/91jd01310, 1992.



- 1 Gruzdev, A. N., and Sitnov, S. A.: Tropospheric Ozone Annual Variation and Possible
2 Troposphere-Stratosphere Coupling in the Arctic and Antarctic as Derived from Ozone Soundings
3 at Resolute and Amundsen-Scott Stations, *Tellus B*, 45, 89-98, DOI 10.1034/j.1600-0889.1993.t01-
4 1-00001.x, 1993.
- 5 Hansen, A. M. K., Kristensen, K., Nguyen, Q. T., Zare, A., Cozzi, F., Nøjgaard, J. K., Skov, H.,
6 Brandt, J., Christensen, J. H., Ström, J., Tunved, P., Krejci, R., and Glasius, M.: Organosulfates and
7 organic acids in Arctic aerosols: speciation, annual variation and concentration levels, *Atmos.*
8 *Chem. Phys. Discuss.*, 14, 4745-4785, 10.5194/acpd-14-4745-2014, 2014.
- 9 Hansen, J., and Nazarenko, L.: Soot climate forcing via snow and ice albedos, *P Natl Acad Sci*
10 *USA*, 101, 423-428, 10.1073/pnas.2237157100, 2004.
- 11 Heidam, N. Z., Wahlin, P., and Christensen, J. H.: Tropospheric gases and aerosols in northeast
12 Greenland, *J Atmos Sci*, 56, 261-278, [http://dx.doi.org/10.1175/1520-](http://dx.doi.org/10.1175/1520-0469(1999)056<0261:TGAAN>2.0.CO;2)
13 [0469\(1999\)056<0261:TGAAN>2.0.CO;2](http://dx.doi.org/10.1175/1520-0469(1999)056<0261:TGAAN>2.0.CO;2), 1999.
- 14 Heidam, N. Z., Christensen, J., Wahlin, P., and Skov, H.: Arctic atmospheric contaminants in NE
15 Greenland: levels, variations, origins, transport, transformations and trends 1990-2001, *Sci Total*
16 *Environ*, 331, 5-28, 10.1016/j.scitotenv.2004.03.033, 2004.
- 17 Heintzenberg, J., Leck, C., and Tunved, P.: Potential source regions and processes of aerosol in the
18 summer Arctic, *Atmos. Chem. Phys.*, 15, 6487-6502, 10.5194/acp-15-6487-2015, 2015.
- 19 Hirdman, D., Sodemann, H., Eckhardt, S., Burkhardt, J. F., Jefferson, A., Mefford, T., Quinn, P. K.,
20 Sharma, S., Strom, J., and Stohl, A.: Source identification of short-lived air pollutants in the Arctic
21 using statistical analysis of measurement data and particle dispersion model output, *Atmos Chem*
22 *Phys*, 10, 669-693, 2010.
- 23 IPCC: Climate Change 2013: The Physical Science Basis. Contribution of Working Group I to the
24 Fifth Assessment Report of the Intergovernmental Panel on Climate Change, Cambridge University
25 Press, Cambridge, United Kingdom and New York, NY, USA, 1535 pp., 2013.
- 26 Kahl, J. D. W., Martinez, D. A., Kuhns, H., Davidson, C. I., Jaffrezo, J. L., and Harris, J. M.: Air
27 mass trajectories to Summit, Greenland: A 44-year climatology and some episodic events, *J*
28 *Geophys Res-Oceans*, 102, 26861-26875, Doi 10.1029/97jc00296, 1997.
- 29 Karl, M., Leck, C., Gross, A., and Pirjola, L.: A study of new particle formation in the marine
30 boundary layer over the central Arctic Ocean using a flexible multicomponent aerosol dynamic
31 model, *Tellus B*, 64, Artn 17158 Doi 10.3402/Tellusb.V64i0.17158, 2012.
- 32 Karl, M., Leck, C., Coz, E., and Heintzenberg, J.: Marine nanogels as a source of atmospheric
33 nanoparticles in the high Arctic, *Geophysical Research Letters*, 40, 3738-3743, Doi
34 10.1002/Grl.50661, 2013.
- 35 Korhonen, H., Carslaw, K. S., Spracklen, D. V., Ridley, D. A., and Strom, J.: A global model study
36 of processes controlling aerosol size distributions in the Arctic spring and summer, *J Geophys Res-*
37 *Atmos*, 113, Artn D08211 Doi 10.1029/2007jd009114, 2008.



- 1 Kristensson, A., Dal Maso, M., Swietlicki, E., Hussein, T., Zhou, J., Kerminen, V. M., and
2 Kulmala, M.: Characterization of new particle formation events at a background site in Southern
3 Sweden: relation to air mass history, *Tellus B*, 60, 330-344, DOI 10.1111/j.1600-
4 0889.2008.00345.x, 2008.
- 5 Kulmala, M., Dal Maso, M., Makela, J. M., Pirjola, L., Vakeva, M., Aalto, P., Miikkulainen, P.,
6 Hameri, K., and O'Dowd, C. D.: On the formation, growth and composition of nucleation mode
7 particles, *Tellus B*, 53, 479-490, DOI 10.1034/j.1600-0889.2001.530411.x, 2001.
- 8 Kwok, R.: Outflow of Arctic Ocean Sea Ice into the Greenland and Barents Seas: 1979-2007, *J*
9 *Climate*, 22, 2438-2457, 10.1175/2008JCLI2819.1, 2009.
- 10 Kyro, E. M., Vaananen, R., Kerminen, V. M., Virkkula, A., Petaja, T., Asmi, A., Dal Maso, M.,
11 Nieminen, T., Juhola, S., Shcherbinin, A., Riipinen, I., Lehtipalo, K., Keronen, P., Aalto, P. P.,
12 Hari, P., and Kulmala, M.: Trends in new particle formation in eastern Lapland, Finland: effect of
13 decreasing sulfur emissions from Kola Peninsula, *Atmos Chem Phys*, 14, 4383-4396, DOI
14 10.5194/acp-14-4383-2014, 2014.
- 15 Law, K. S., and Stohl, A.: Arctic air pollution: Origins and impacts, *Science*, 315, 1537-1540, DOI
16 10.1126/science.1137695, 2007.
- 17 Leaitch, W. R., Sharma, S., Huang, L., Toom-Saunty, D., Chivulescu, A., Macdonald, A. M.,
18 Salzen, K. v., Pierce, J. R., Bertram, A. K., Schroder, J. C., Shantz, N. C., Chang, R. Y. W., and
19 Norman, A. L.: Dimethyl sulfide control of the clean summertime Arctic aerosol and cloud, *Elem.*
20 *Sci. Anth.*, 1, 10.12952/journal.elementa.000017, 2013.
- 21 Leck, C., Norman, M., Bigg, E. K., and Hillamo, R.: Chemical composition and sources of the high
22 Arctic aerosol relevant for cloud formation, *J Geophys Res-Atmos*, 107, Artn 4135 Doi
23 10.1029/2001jc001463, 2002.
- 24 Li, S. M., and Barrie, L. A.: Biogenic Sulfur Aerosol in the Arctic Troposphere .1. Contributions to
25 Total Sulfate, *J Geophys Res-Atmos*, 98, 20613-20622, 10.1029/93JD02234, 1993.
- 26 Mahajan, A. S., Sorribas, M., Martin, J. C. G., MacDonald, S. M., Gil, M., Plane, J. M. C., and
27 Saiz-Lopez, A.: Concurrent observations of atomic iodine, molecular iodine and ultrafine particles
28 in a coastal environment, *Atmos Chem Phys*, 11, 2545-2555, 10.5194/acp-11-2545-2011, 2011.
- 29 Markus, T., Stroeve, J. C., and Miller, J.: Recent changes in Arctic sea ice melt onset, freezeup, and
30 melt season length, *J Geophys Res-Oceans*, 114, Artn C12024 Doi 10.1029/2009jc005436, 2009.
- 31 Massling, A., Nielsen, I. E., Kristensen, D., Christensen, J. H., Sørensen, L. L., Jensen, B., Nguyen,
32 Q. T., Nøjgaard, J. K., Glasius, M., and Skov, H.: Atmospheric black carbon and sulfate
33 concentrations in Northeast Greenland, *Atmos. Chem. Phys.*, 15, 9681-9692, 10.5194/acp-15-9681-
34 2015, 2015.
- 35 McFiggans, G., Bale, C. S. E., Ball, S. M., Beames, J. M., Bloss, W. J., Carpenter, L. J., Dorsey, J.,
36 Dunk, R., Flynn, M. J., Furneaux, K. L., Gallagher, M. W., Heard, D. E., Hollingsworth, A. M.,
37 Hornsby, K., Ingham, T., Jones, C. E., Jones, R. L., Kramer, L. J., Langridge, J. M., Leblanc, C.,
38 LeCrane, J. P., Lee, J. D., Leigh, R. J., Longley, I., Mahajan, A. S., Monks, P. S., Oetjen, H., Orr-
39 Ewing, A. J., Plane, J. M. C., Potin, P., Shillings, A. J. L., Thomas, F., von Glasow, R., Wada, R.,



- 1 Whalley, L. K., and Whitehead, J. D.: Iodine-mediated coastal particle formation: an overview of
2 the Reactive Halogens in the Marine Boundary Layer (RHAMBLE) Roscoff coastal study, Atmos
3 Chem Phys, 10, 2975-2999, 10.5194/acp-10-2975-2010, 2010.
- 4 Middlebrook, A. M., Murphy, D. M., and Thomson, D. S.: Observations of organic material in
5 individual marine particles at Cape Grim during the First Aerosol Characterization Experiment
6 (ACE 1), J Geophys Res-Atmos, 103, 16475-16483, Doi 10.1029/97jd03719, 1998.
- 7 Monks, P. S.: A review of the observations and origins of the spring ozone maximum, Atmos
8 Environ, 34, 3545-3561, Doi 10.1016/S1352-2310(00)00129-1, 2000.
- 9 Mäkelä, J. M., Maso, M. D., Pirjola, L., Keronen, P., Laakso, L., Kulmala, M., and Laaksonen, A.:
10 Characteristics of the atmospheric particle formation events observed at a boreal forest site in
11 Southern Finland, Boreal Environment Research, 5, 299-313, 2000.
- 12 Nguyen, Q. T., Skov, H., Sørensen, L. L., Jensen, B. J., Grube, A. G., Massling, A., Glasius, M.,
13 and Nøjgaard, J. K.: Source apportionment of particles at Station Nord, North East Greenland
14 during 2008–2010 using COPREM and PMF analysis, Atmos Chem Phys, 13, 35-49, 10.5194/acp-
15 13-35-2013, 2013.
- 16 Nguyen, Q. T., Kristensen, T. B., Hansen, A. M. K., Skov, H., Bossi, R., Massling, A., Sorensen, L.
17 L., Bilde, M., Glasius, M., and Nøjgaard, J. K.: Characterization of humic-like substances in Arctic
18 aerosols, J Geophys Res-Atmos, 119, 5011-5027, Doi 10.1002/2013jd020144, 2014.
- 19 O'Dowd, C. D., Hameri, K., Makela, J. M., Pirjola, L., Kulmala, M., Jennings, S. G., Berresheim,
20 H., Hansson, H. C., de Leeuw, G., Kunz, G. J., Allen, A. G., Hewitt, C. N., Jackson, A., Viisanen,
21 Y., and Hoffmann, T.: A dedicated study of New Particle Formation and Fate in the Coastal
22 Environment (PARFORCE): Overview of objectives and achievements, J Geophys Res-Atmos,
23 107, 10.1029/2001jd000555, 2002.
- 24 Odowd, C. D., and Smith, M. H.: Physicochemical Properties of Aerosols over the Northeast
25 Atlantic - Evidence for Wind-Speed-Related Submicron Sea-Salt Aerosol Production, J Geophys
26 Res-Atmos, 98, 1137-1149, Doi 10.1029/92jd02302, 1993.
- 27 Pfeifer, S., Birmili, W., Schladitz, A., Muller, T., Nowak, A., and Wiedensohler, A.: A fast and
28 easy-to-implement inversion algorithm for mobility particle size spectrometers considering particle
29 number size distribution information outside of the detection range, Atmos Meas Tech, 7, 95-105,
30 10.5194/amt-7-95-2014, 2014.
- 31 Pirjola, L., O'Dowd, C. D., Brooks, I. M., and Kulmala, M.: Can new particle formation occur in the
32 clean marine boundary layer?, J Geophys Res-Atmos, 105, 26531-26546, Doi
33 10.1029/2000jd900310, 2000.
- 34 Pnyushkov, A. V., Polyakov, I. V., Ivanov, V. V., and Kikuchi, T.: Structure of the Fram Strait
35 branch of the boundary current in the Eurasian Basin of the Arctic Ocean, Polar Sci, 7, 53-71,
36 10.1016/j.polar.2013.02.001, 2013.
- 37 Pratt, K. A., Custard, K. D., Shepson, P. B., Douglas, T. A., Pohler, D., General, S., Zielcke, J.,
38 Simpson, W. R., Platt, U., Tanner, D. J., Gregory Huey, L., Carlsen, M., and Stirm, B. H.:



- 1 Photochemical production of molecular bromine in Arctic surface snowpacks, *Nature Geosci*, 6,
2 351-356, 10.1038/ngeo1779 2013.
- 3 Pryor, S. C., Spaulding, A. M., and Barthelmie, R. J.: New particle formation in the Midwestern
4 USA: Event characteristics, meteorological context and vertical profiles, *Atmos Environ*, 44, 4413-
5 4425, DOI 10.1016/j.atmosenv.2010.07.045, 2010.
- 6 Quinn, P. K., Miller, T. L., Bates, T. S., Ogren, J. A., Andrews, E., and Shaw, G. E.: A 3-year
7 record of simultaneously measured aerosol chemical and optical properties at Barrow, Alaska, *J*
8 *Geophys Res-Atmos*, 107, Doi 10.1029/2001jd001248, 2002.
- 9 Quinn, P. K., Bates, T. S., Baum, E., Doubleday, N., Fiore, A. M., Flanner, M., Fridlind, A.,
10 Garrett, T. J., Koch, D., Menon, S., Shindell, D., Stohl, A., and Warren, S. G.: Short-lived
11 pollutants in the Arctic: their climate impact and possible mitigation strategies, *Atmos Chem Phys*,
12 8, 1723-1735, DOI 10.5194/acp-8-1723-2008, 2008.
- 13 Riipinen, I., Pierce, J. R., Yli-Juuti, T., Nieminen, T., Hakkinen, S., Ehn, M., Junninen, H.,
14 Lehtipalo, K., Petaja, T., Slowik, J., Chang, R., Shantz, N. C., Abbatt, J., Leaitch, W. R., Kerminen,
15 V. M., Worsnop, D. R., Pandis, S. N., Donahue, N. M., and Kulmala, M.: Organic condensation: a
16 vital link connecting aerosol formation to cloud condensation nuclei (CCN) concentrations, *Atmos*
17 *Chem Phys*, 11, 3865-3878, DOI 10.5194/acp-11-3865-2011, 2011.
- 18 Riipinen, I., Yli-Juuti, T., Pierce, J. R., Petaja, T., Worsnop, D. R., Kulmala, M., and Donahue, N.
19 M.: The contribution of organics to atmospheric nanoparticle growth, *Nat Geosci*, 5, 453-458, Doi
20 10.1038/Ngeo1499, 2012.
- 21 Saiz-Lopez, A., and von Glasow, R.: Reactive halogen chemistry in the troposphere, *Chem Soc*
22 *Rev*, 41, 6448-6472, 10.1039/c2cs35208g, 2012.
- 23 Sellegri, K., O'Dowd, C. D., Yoon, Y. J., Jennings, S. G., and de Leeuw, G.: Surfactants and
24 submicron sea spray generation, *J Geophys Res-Atmos*, 111, Artn D22215 Doi
25 10.1029/2005jd006658, 2006.
- 26 Shupe, M. D., and Intrieri, J. M.: Cloud radiative forcing of the Arctic surface: The influence of
27 cloud properties, surface albedo, and solar zenith angle, *J Climate*, 17, 616-628, Doi 10.1175/1520-
28 0442(2004)017<0616:Crfota>2.0.Co;2, 2004.
- 29 Simpson, W. R., von Glasow, R., Riedel, K., Anderson, P., Ariya, P., Bottenheim, J., Burrows, J.,
30 Carpenter, L. J., Friess, U., Goodsite, M. E., Heard, D., Hutterli, M., Jacobi, H. W., Kaleschke, L.,
31 Neff, B., Plane, J., Platt, U., Richter, A., Roscoe, H., Sander, R., Shepson, P., Sodeau, J., Steffen,
32 A., Wagner, T., and Wolff, E.: Halogens and their role in polar boundary-layer ozone depletion,
33 *Atmos Chem Phys*, 7, 4375-4418, 2007.
- 34 Singh, H. B., Kanakidou, M., Crutzen, P. J., and Jacob, D. J.: High-Concentrations and
35 Photochemical Fate of Oxygenated Hydrocarbons in the Global Troposphere, *Nature*, 378, 50-54,
36 Doi 10.1038/378050a0, 1995.
- 37 Skov, H., Christensen, J. H., Goodsite, M. E., Heidam, N. Z., Jensen, B., Wahlin, P., and Geernaert,
38 G.: Fate of elemental mercury in the arctic during atmospheric mercury depletion episodes and the



- 1 load of atmospheric mercury to the arctic, *Environ Sci Technol*, 38, 2373-2382,
2 10.1021/es030080h, 2004.
- 3 Stendel, M., Christensen, J. H., and Petersen, D.: Arctic climate and climate change with a focus on
4 Greenland, *Adv Ecol Res*, 40, 13-43, 10.1016/S0065-2504(07)00002-5, 2008.
- 5 Stroeve, J., Serreze, M., Holland, M., Kay, J., Malanik, J., and Barrett, A.: The Arctic's rapidly
6 shrinking sea ice cover: a research synthesis, *Climatic Change*, 110, 1005-1027, 10.1007/s10584-
7 011-0101-1, 2012.
- 8 Ström, J., Umegard, J., Torseth, K., Tunved, P., Hansson, H. C., Holmen, K., Wismann, V., Herber,
9 A., and König-Langlo, G.: One year of particle size distribution and aerosol chemical composition
10 measurements at the Zeppelin Station, Svalbard, March 2000-March 2001, *Physics and Chemistry
11 of the Earth*, 28, 1181-1190, DOI 10.1016/j.pce.2003.08.058, 2003.
- 12 Tervahattu, H., Juhanoja, J., and Kupiainen, K.: Identification of an organic coating on marine
13 aerosol particles by TOF-SIMS, *J Geophys Res-Atmos*, 107, Artn 4319 Doi
14 10.1029/2001jd001403, 2002.
- 15 Tunved, P., Ström, J., and Krejci, R.: Arctic aerosol life cycle: linking aerosol size distributions
16 observed between 2000 and 2010 with air mass transport and precipitation at Zeppelin station, Ny-
17 Ålesund, Svalbard, *Atmos. Chem. Phys.*, 13, 3643-3660, 10.5194/acp-13-3643-2013, 2013.
- 18 Vehkamäki, H., Dal Maso, M., Hussein, T., Flanagan, R., Hyvärinen, A., Lauros, J., Merikanto, J.,
19 Monkkonen, P., Pihlatie, M., Salminen, K., Sogacheva, L., Thum, T., Ruuskanen, T. M., Keronen,
20 P., Aalto, P. P., Hari, P., Lehtinen, K. E. J., Rannik, U., and Kulmala, M.: Atmospheric particle
21 formation events at Varrio measurement station in Finnish Lapland 1998-2002, *Atmos Chem Phys*,
22 4, 2015-2023, 2004.
- 23 Vaananen, R., Kyro, E. M., Nieminen, T., Kivekas, N., Junninen, H., Virlikula, A., Dal Maso, M.,
24 Lihavainen, H., Viisanen, Y., Svenningsson, B., Holst, T., Arneth, A., Aalto, P. P., Kulmala, M.,
25 and Kerminen, V. M.: Analysis of particle size distribution changes between three measurement
26 sites in northern Scandinavia, *Atmos Chem Phys*, 13, 11887-11903, DOI 10.5194/acp-13-11887-
27 2013, 2013.
- 28 Walker, T. W., Jones, D. B. A., Parrington, M., Henze, D. K., Murray, L. T., Bottenheim, J. W.,
29 Anlauf, K., Worden, J. R., Bowman, K. W., Shim, C., Singh, K., Kopacz, M., Tarasick, D. W.,
30 Davies, J., von der Gathen, P., Thompson, A. M., and Carouge, C. C.: Impacts of midlatitude
31 precursor emissions and local photochemistry on ozone abundances in the Arctic, *J Geophys Res-
32 Atmos*, 117, Artn D01305 Doi 10.1029/2011jd016370, 2012.
- 33 Wiedensohler, A., Covert, D. S., Swietlicki, E., Aalto, P., Heintzenberg, J., and Leck, C.:
34 Occurrence of an ultrafine particle mode less than 20 nm in diameter in the marine boundary layer
35 during Arctic summer and autumn, *Tellus B*, 48, 213-222, DOI 10.1034/j.1600-0889.1996.t01-1-
36 00006.x, 1996.
- 37 Wiedensohler, A., Birmili, W., Nowak, A., Sonntag, A., Weinhold, K., Merkel, M., Wehner, B.,
38 Tuch, T., Pfeifer, S., Fiebig, M., Fjaraa, A. M., Asmi, E., Sellegri, K., Depuy, R., Venzac, H.,
39 Villani, P., Laj, P., Aalto, P., Ogren, J. A., Swietlicki, E., Williams, P., Roldin, P., Quincey, P.,



- 1 Huglin, C., Fierz-Schmidhauser, R., Gysel, M., Weingartner, E., Riccobono, F., Santos, S.,
- 2 Gruning, C., Faloon, K., Beddows, D., Harrison, R. M., Monahan, C., Jennings, S. G., O'Dowd, C.
- 3 D., Marinoni, A., Horn, H. G., Keck, L., Jiang, J., Scheckman, J., McMurry, P. H., Deng, Z., Zhao,
- 4 C. S., Moerman, M., Henzing, B., de Leeuw, G., Loschau, G., and Bastian, S.: Mobility particle size
- 5 spectrometers: harmonization of technical standards and data structure to facilitate high quality
- 6 long-term observations of atmospheric particle number size distributions, *Atmos Meas Tech*, 5,
- 7 657-685, DOI 10.5194/amt-5-657-2012, 2012.

- 8 Winklmayr, W., Reischl, G. P., Lindner, A. O., and Berner, A.: A New Electromobility
- 9 Spectrometer for the Measurement of Aerosol Size Distributions in the Size Range from 1 to 1000
- 10 Nm, *J Aerosol Sci*, 22, 289-296, 1991.

- 11 Ziemba, L. D., Dibb, J. E., Griffin, R. J., Huey, L. G., and Beckman, P.: Observations of particle
- 12 growth at a remote, Arctic site, *Atmos Environ*, 44, 1649-1657, DOI
- 13 10.1016/j.atmosenv.2010.01.032, 2010.

- 14 Zwally, H. J., Abdalati, W., Herring, T., Larson, K., Saba, J., and Steffen, K.: Surface melt-induced
- 15 acceleration of Greenland ice-sheet flow, *Science*, 297, 218-222, DOI 10.1126/science.1072708,
- 16 2002.

- 17



1 **List of Figures**

2 **Fig. 1.** The high Arctic site Villum Research Station, Station Nord (81°36' N, 16°40'W, 30 m a.s.l.)
3 in northeast Greenland. The main measurement site is Flyger's hut, which is located about 2.5 km
4 southeast of the Danish military base.

5 **Fig. 2.** SMPS, O₃ and NO_x data coverage at Station Nord from July 2010 - February 2013.

6 **Fig. 3.** Time series of particle number size distributions as dN/dlogDp (cm⁻³) during 2012. The
7 original 5 min time resolution was used in the plots.

8 **Fig. 4.** Monthly median particle number size distribution at Station Nord during 2012. The
9 corresponding lognormal-fitting parameters are shown in **Table 2**.

10 **Fig. 5.** Windroses showing monthly wind direction and wind speed at Station Nord during 2012.
11 The concentric rings show the percentage of wind arriving from a particular direction.

12 **Fig. 6.** Demonstration of the impacts of O₃, NO and NO_x on the summer new particle formation
13 events occurring on June 15-20 (Event A), Aug 2 (Event B) and Aug 9-10 (Event C) in 2012.

14 **Fig. 7.** Demonstration of air mass back trajectories calculated using HYSPLIT for arrival at 50 m
15 and 500 m at the station on selected days with new particle formation events.

16 **Fig. 8.** The probability of observing an event at Station Nord (bottom tip of the black triangle) as a
17 function of air mass origin.

18 **Fig. 9.** Monthly variation of total number of days with good data (left vertical axis) and frequency
19 percentages (%) of event days, non-event days and undefined days (right vertical axis) during the
20 study period (July 2010 - February 2013).

21

22

23



1 **List of Tables**

2 **Table 1.** Three modes were fitted to the average monthly data of 2012 using lognormal fitting. The
3 parameters shown for each mode include the modal number concentration (N , cm^{-3}), the modal
4 geometrical mean diameter (D_g , nm) and the modal geometrical standard deviation (GSD). **Table 2.**
5 Three modes were fitted to the average data for each month of 2012 using lognormal fitting. The
6 parameters shown for each mode include the modal number concentration (N , cm^{-3}), the modal
7 geometrical mean diameter (D_g , nm) and the modal geometrical standard deviation (GSD).

8 **Table 2.** Median and average particle number concentration (N), particle volume concentration (V)
9 and particle mass concentration (M) for the 12 months of 2012. M was calculated from V assuming
10 a density of 1.4 g cm^{-3} and particle sphericity.

11 **Table 3.** Percentage of total new particle formation events (marked in blue) versus non-events and
12 undefined days during the period July 2010 to February 2013. The total events were further divided
13 into Class I and Class II events. A column of total days (by month) over the studied years was also
14 provided.

15

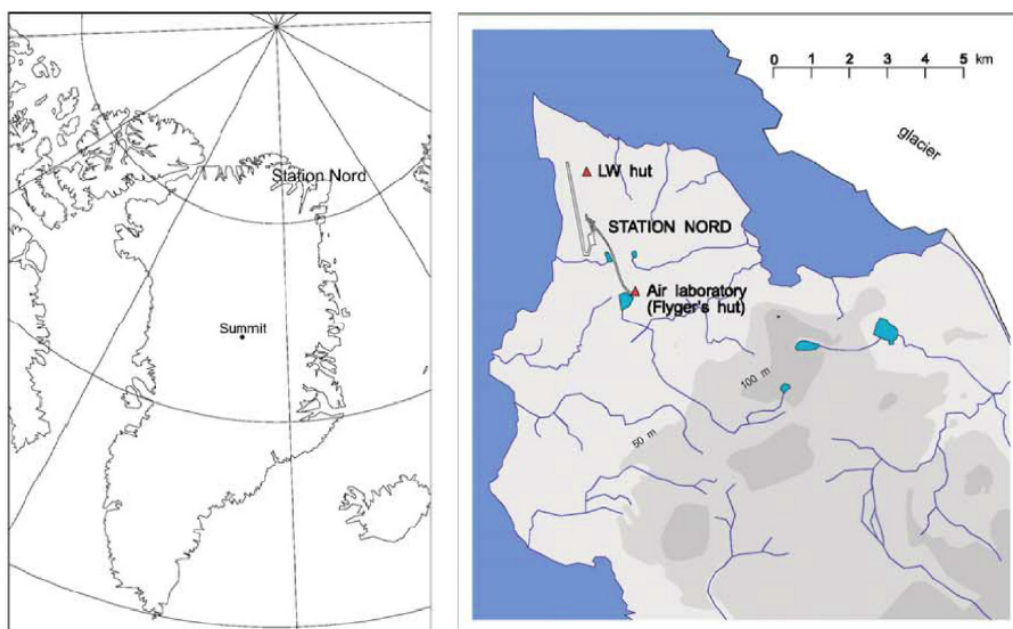
16

17



1 Figures

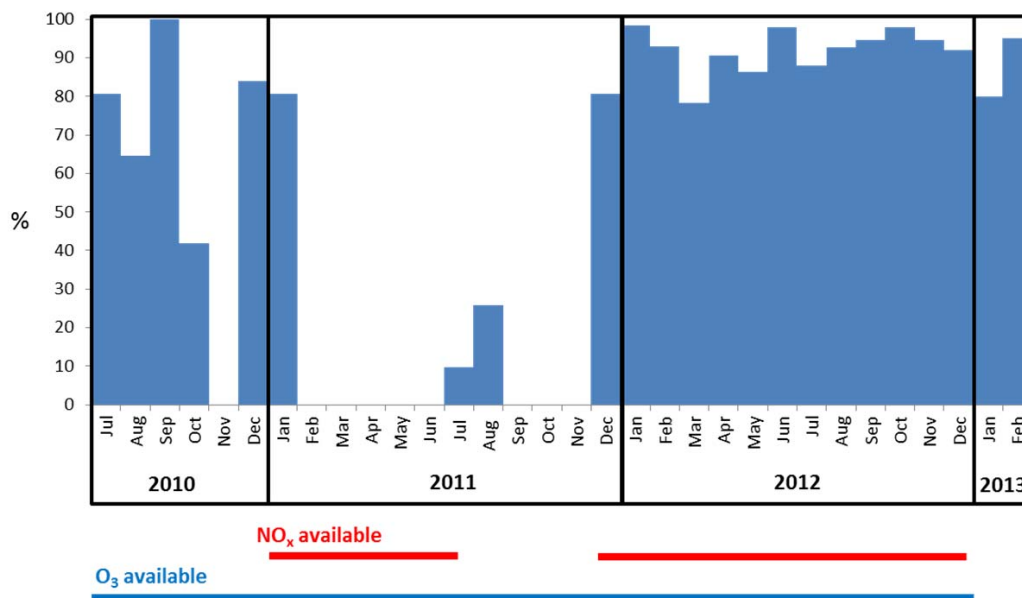
- 2 **Fig. 1.** The high Arctic site Villum Research Station, Station Nord (81°36' N, 16°40' W, 30 m a.s.l.)
3 in northeast Greenland. The main measurement site is Flyger's hut, which is located about 2.5 km
4 southeast of the Danish military base.



5
6



1 **Fig. 2.** SMPS, O₃ and NO_x data coverage at Station Nord from July 2010 - February 2013.

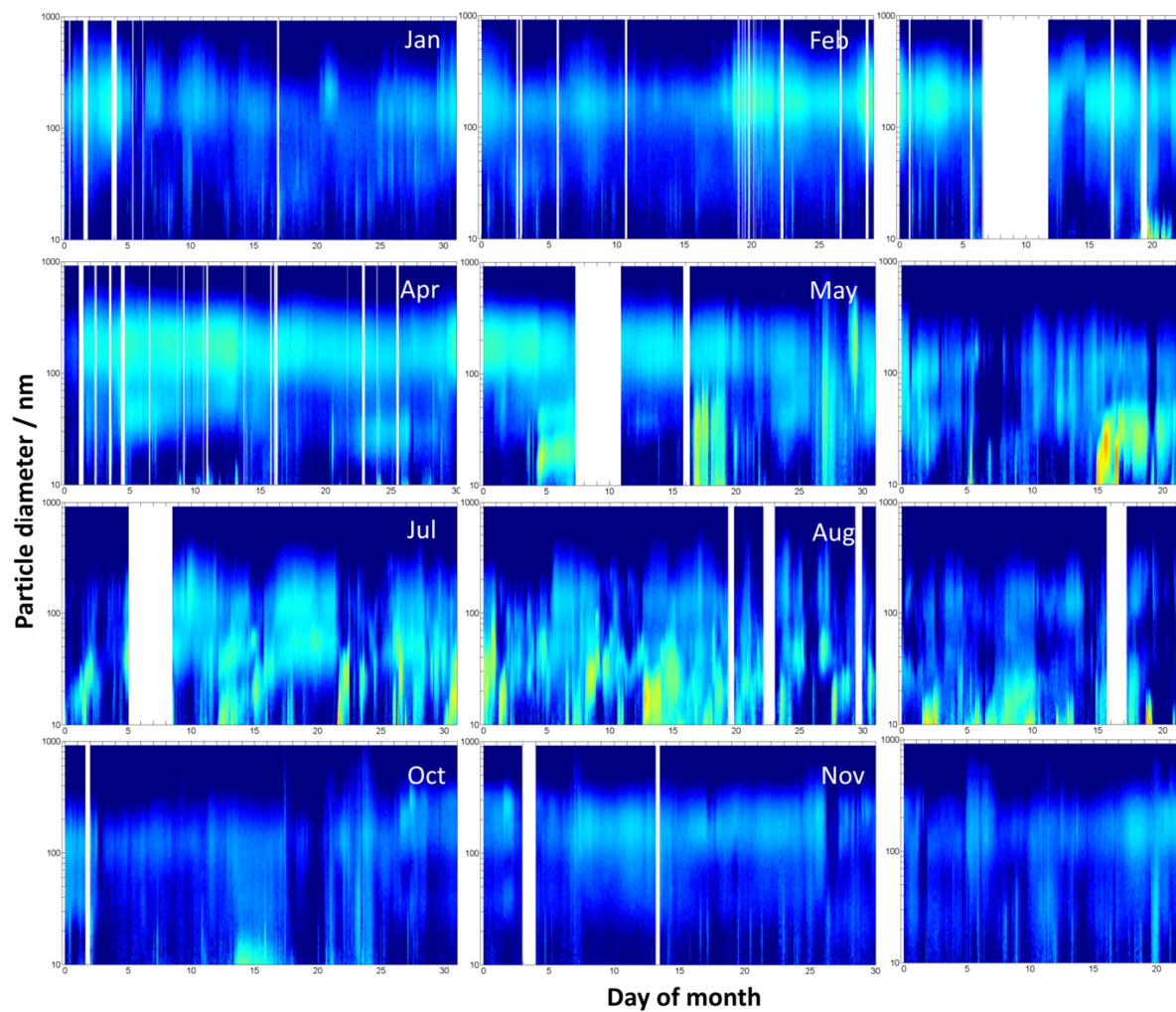


2

3



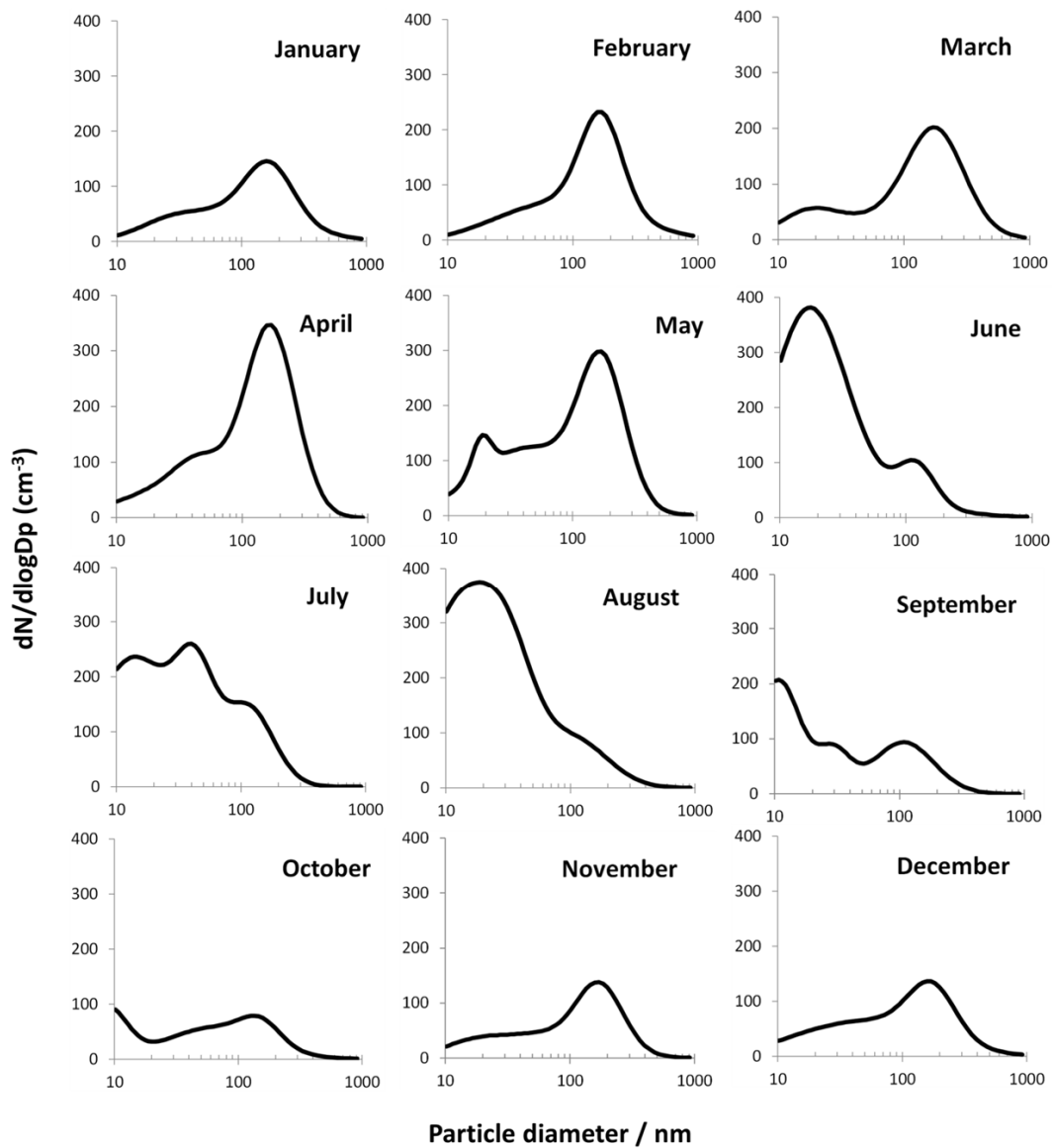
1 **Fig. 3.** Time series of particle number size distributions as $dN/d\log D_p$ (cm^{-3}) during 2012. The
2 original 5 min time resolution was used in the plots.
3



4
5



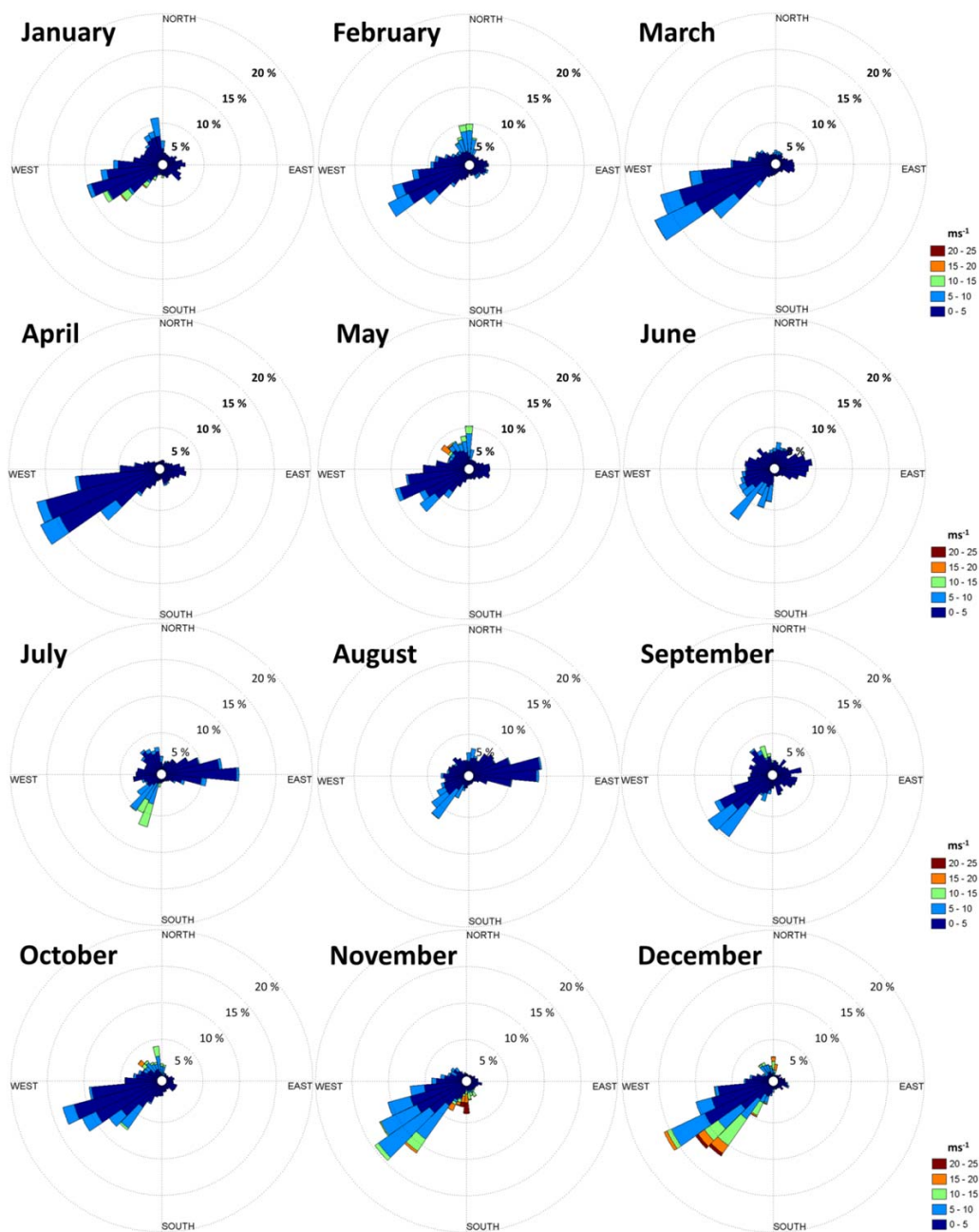
1 **Fig. 4.** Monthly median particle number size distribution at Station Nord during 2012. The
2 corresponding lognormal-fitting parameters are shown in **Table 2.**
3



4
5



- 1 **Fig. 5.** Windroses showing monthly wind direction and wind speed at Station Nord during 2012.
- 2 The concentric rings show the percentage of wind arriving from a particular direction.

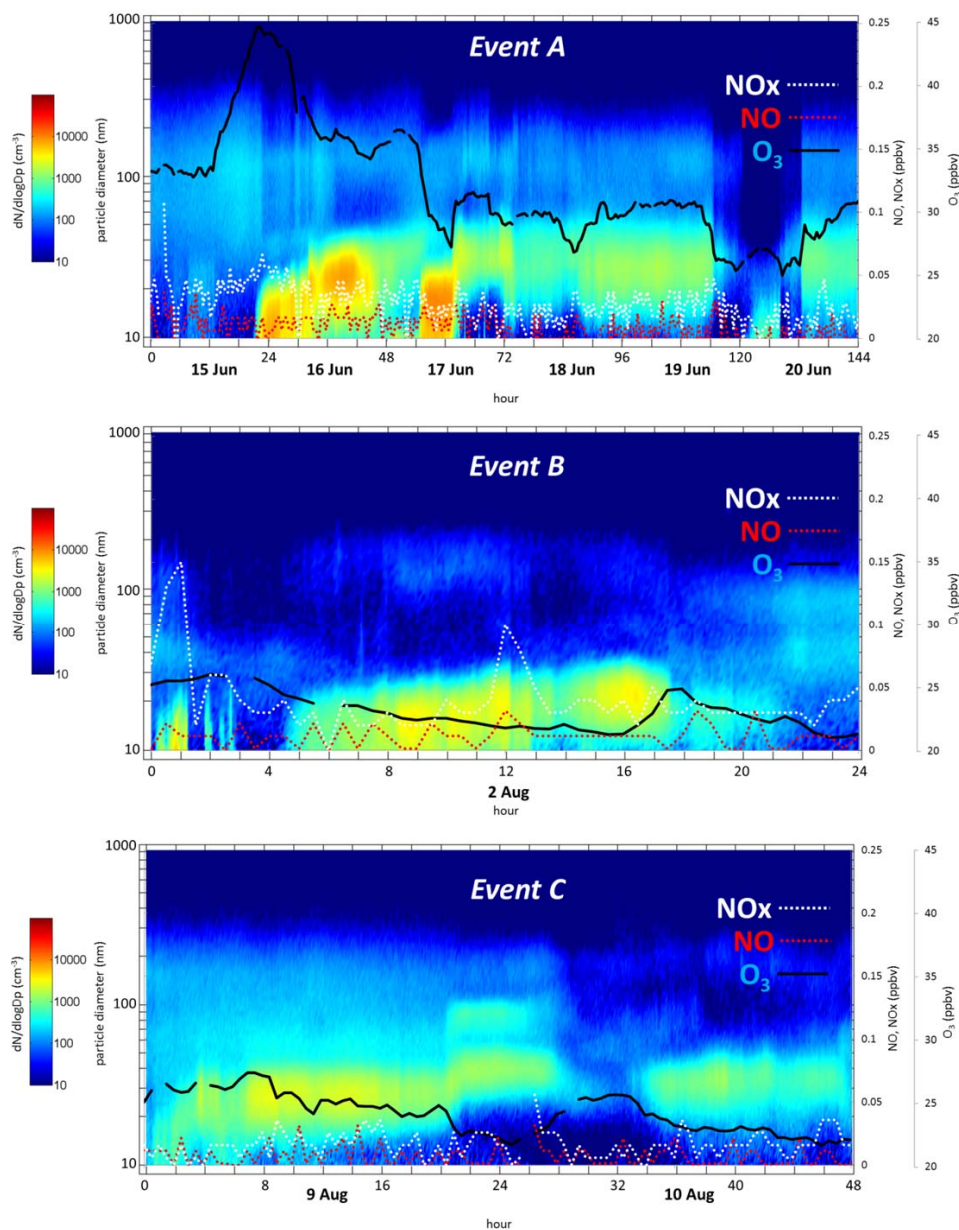


3



1 **Fig. 6.** Demonstration of the connection between O₃, NO and NO_x and summertime new particle
2 formation events occurring on June 15-20 (Event A), Aug 2 (Event B) and Aug 9-10 (Event C) in
3 2012.

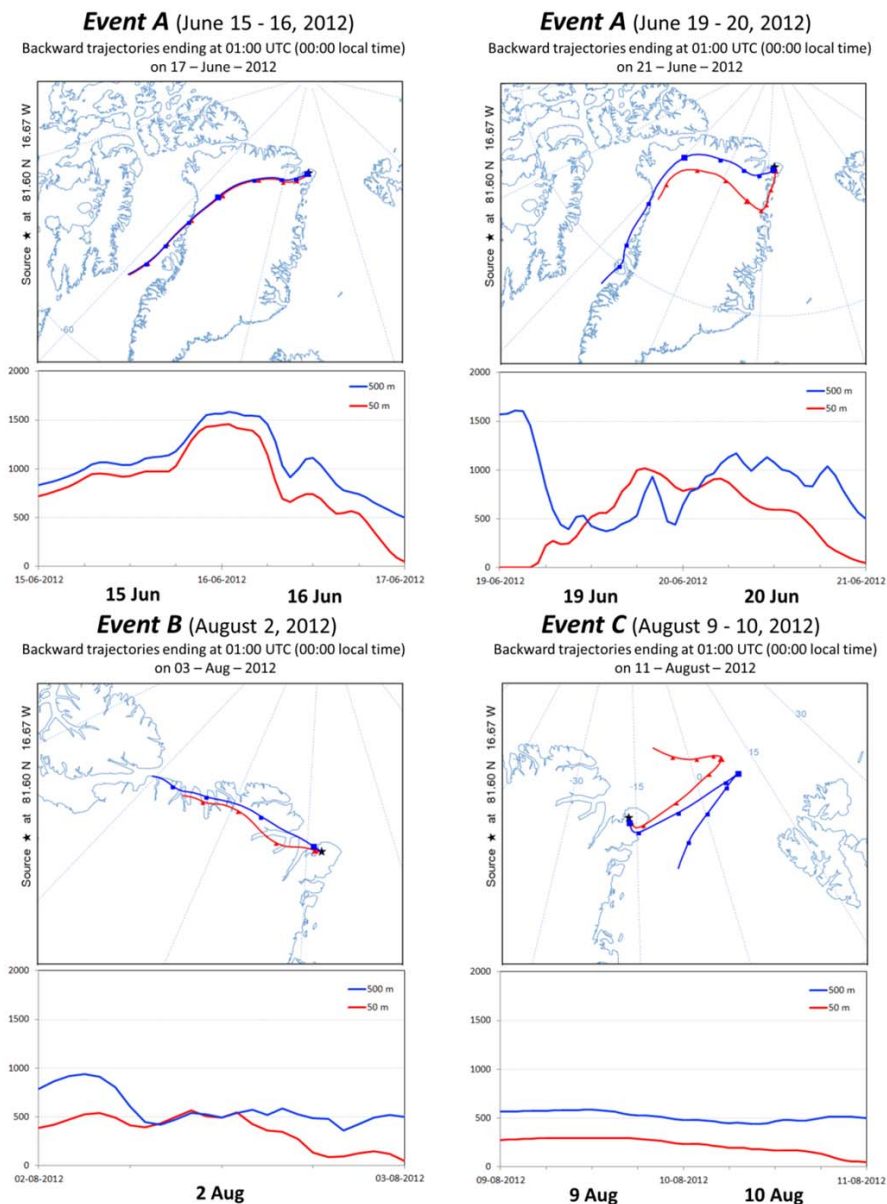
4



5



1 **Fig. 7.** Demonstration of air mass back trajectories calculated using HYSPLIT for arrival at 50 m
2 and 500 m at the station on selected days with new particle formation events.



3

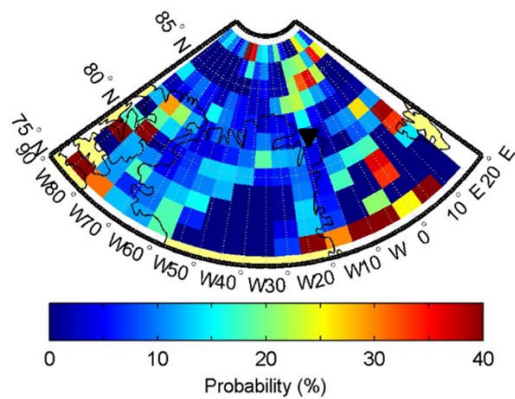
4

5

6



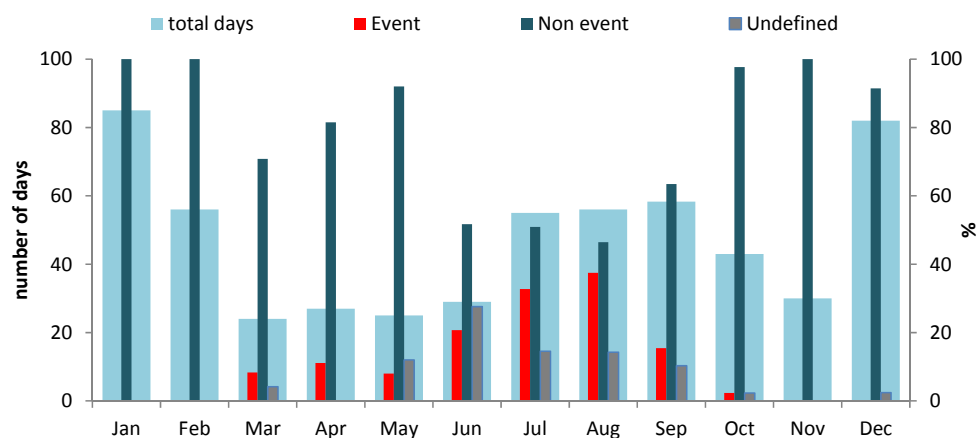
- 1 **Fig. 8.** The probability of observing an event at Station Nord (bottom tip of the black triangle) as a
- 2 function of air mass origin.
- 3



- 4
- 5



1 **Fig. 9.** Monthly variation of total number of days with good data (left vertical axis) and frequency
2 percentages (%) of event days, non-event days and undefined days (right vertical axis) during the
3 study period (July 2010 - February 2013).



4
5
6



1 **Table**

2 **Table 1.** Three modes were fitted to the average monthly data of 2012 using lognormal fitting. The
 3 parameters shown for each mode include the modal number concentration (N , cm^{-3}), the modal
 4 geometrical mean diameter (D_g , nm) and the modal geometrical standard deviation (GSD).

	N_1 (cm^{-3})	$D_{g,1}$ (nm)	GSD ₁	N_2 (cm^{-3})	$D_{g,2}$ (nm)	GSD ₂	N_3 (cm^{-3})	$D_{g,3}$ (nm)	GSD ₃
January	5	22	1.4	72	68	3.3	50	167	1.6
February	22	27	2.2	58	97	2.7	75	169	1.5
March	24	17	1.7	49	84	2.8	93	179	1.7
April	45	24	2.4	38	48	1.6	172	167	1.6
May	17	18	1.2	134	43	2.5	125	173	1.5
June	252	17	1.9	22	31	1.4	45	113	1.5
July	196	21	2.6	24	45	1.3	50	119	1.6
August	287	16	2.3	51	30	1.5	49	114	1.8
September	90	11	1.5	25	29	1.4	57	107	1.8
October	25	9	1.3	60	41	3.3	24	139	1.5
November	12	16	1.7	45	62	2.6	51	173	1.5
December	31	22	2.4	48	100	2.5	35	170	1.5

5

6



- 1 **Table 2.** Median and average particle number concentration (N), particle volume concentration (V)
2 and particle mass concentration (M) for the 12 months of 2012. M was calculated from V assuming
3 a density of 1.4 g cm^{-3} and particle sphericity.

	Median N (cm^{-3})	Average N (cm^{-3})	Median V ($\mu\text{m}^3 \text{ cm}^{-3}$)	Average V ($\mu\text{m}^3 \text{ cm}^{-3}$)	Median M ($\mu\text{g m}^{-3}$)	Average M ($\mu\text{g m}^{-3}$)
January	104	121	0.44	0.69	0.61	0.96
February	123	149	0.69	0.82	0.97	1.15
March	170	174	1.10	1.13	1.54	1.58
April	231	253	0.88	0.93	1.24	1.30
May	221	268	0.78	0.78	1.09	1.09
June	137	277	0.14	0.15	0.20	0.21
July	229	237	0.17	0.20	0.23	0.29
August	227	313	0.19	0.21	0.27	0.29
September	124	137	0.18	0.18	0.25	0.25
October	71	87	0.17	0.25	0.24	0.35
November	96	100	0.40	0.42	0.55	0.59
December	85	107	0.30	0.57	0.42	0.80

4

5

6

7



- 1 **Table 3.** Percentage of total new particle formation events (marked in blue) versus non-events and
 2 undefined days during the period July 2010 to February 2013. The total events were further divided
 3 into Class I and Class II events. A column of total days (by month) over the studied years was also
 4 provided.

	Total days	Class I (%)	Class II (%)	Total events (%)	Non-events (%)	Undefined (%)
January	85	0	0	0	100	0
February	56	0	0	0	100	0
March	24	0	8	8	71	4
April	27	0	11	11	81	0
May	25	0	8	8	92	12
June	29	7	14	21	52	28
July	55	9	24	33	51	15
August	56	9	29	38	46	14
September	58	5	10	15	63	10
October	43	0	2	2	98	2
November	30	0	0	0	100	0
December	82	0	0	0	91	2
Total	570	3	9	11	79	7

5

6

7